Les Houches, 18-22 June

How Cosmology Constrains Neutrino Oscillations

Daniela P. Kirilova
Institute of Astronomy, Bulgarian Academy of Sciences, Sofia, Bulgaria

Neutrino oscillations in the early Universe

Big Bang Nucleosynthesis with neutrino oscillations

Updated cosmological constraints on neutrino oscillations

oscillations - asymmetry interplay
relaxation of BBN constraints

D.K., Mihail Chizhov, Nucl. Phys. B, 591 (2000) 457
D.K., M. Chizhov, Nucl. Phys. Suppl. 100, 360 (2001)
D.K., M. Chizhov, astro-ph/0101083, 2001

D.K, M.Ch., Phys. Rev. D 58 (1998) 073004
D.K., M.Ch., Nucl. Phys. B 534 (1998) 447

The evolution of electron neutrino depletion due to $\nu_e \leftrightarrow \nu_s$ oscillations, $\delta m^2 > 0$.

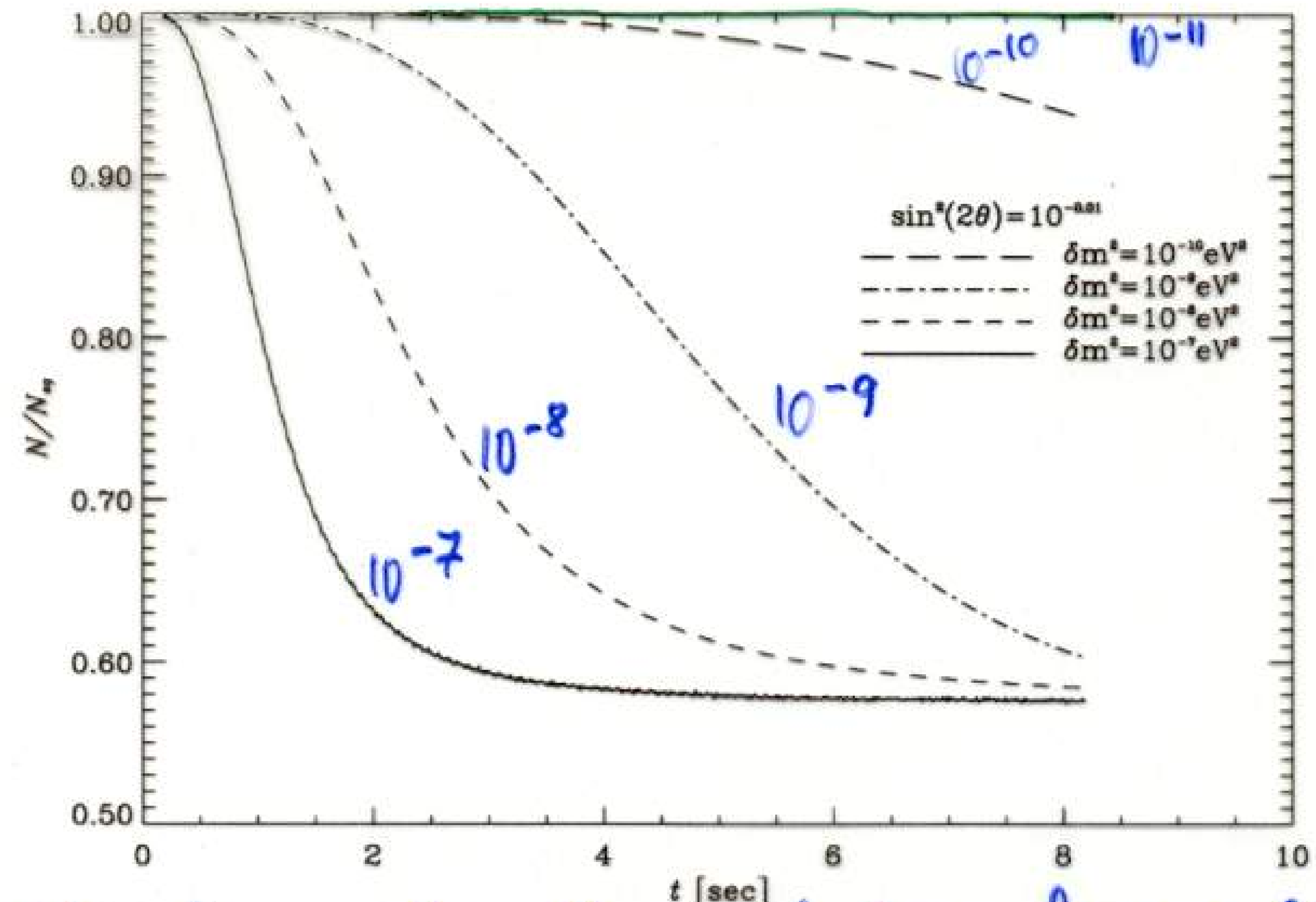

Neutrino density evolution for $\sin^2 2\theta = 0.98$ and different δm^2.

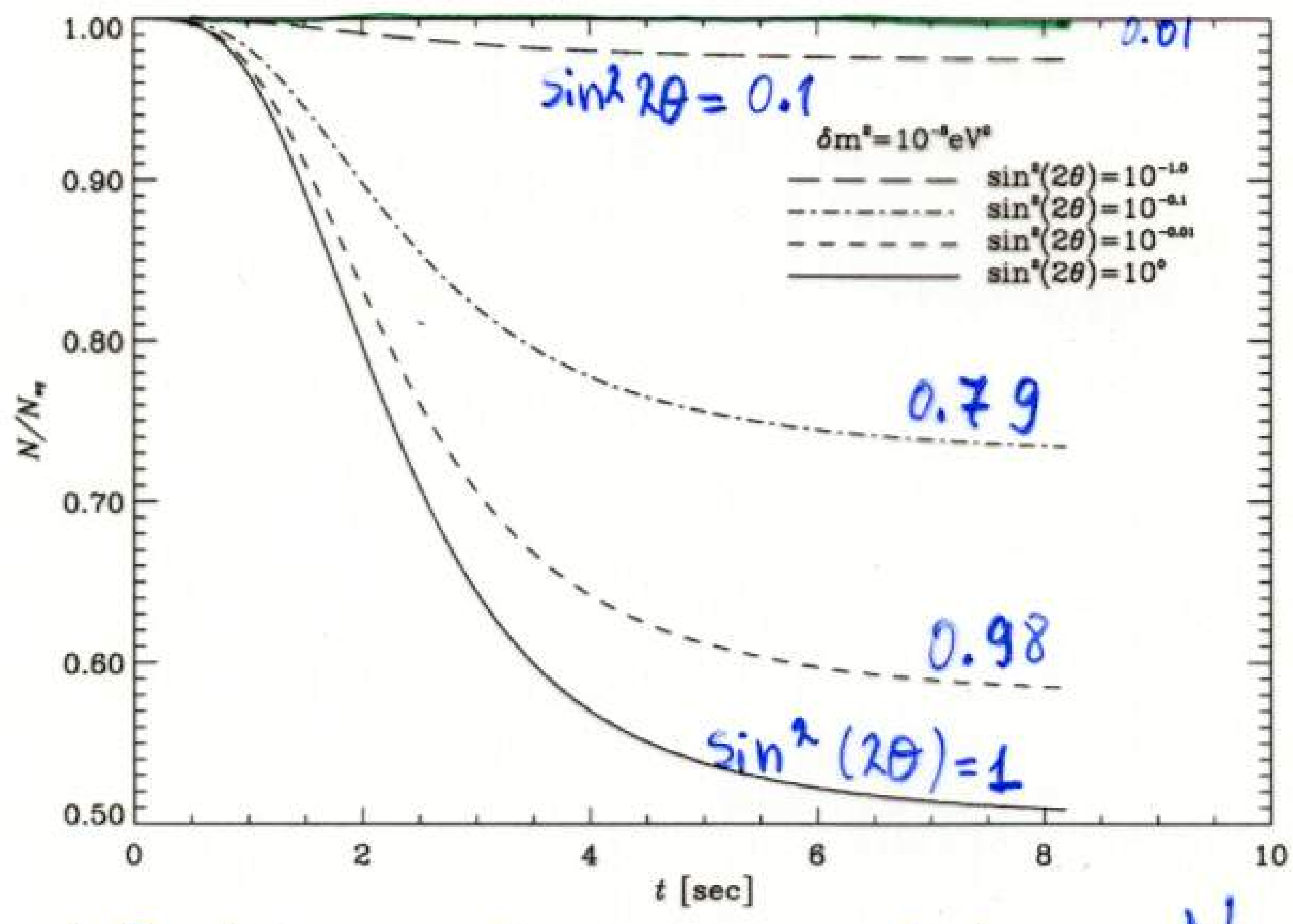

Neutrino density evolution $\frac{N_{\nu_e}}{N_{eq}}(t)$ for $\delta m^2 = 10^{-8}\, eV^2$ and different mixings

The oscillations effect depends on the type of oscillations: oscillation channels, resonant transitions, the degree of equilibrium of oscillating neutrinos.

Neutrino oscillations may

(i) excite additional light particles into equilibrium $N_\nu \uparrow \Rightarrow \Gamma_{exp} \uparrow$

(ii) deplete the neutrino number density $n_{\nu_e} \downarrow \Rightarrow$ modify BBN

(iii) distort the neutrino energy spectrum and BBN

(iv) affect neutrino-antineutrino asymmetry produce erase

All these may play crucial role for neutrino involved processes in the early Universe.

From the allowed range of the observables of our Universe, baryonic density, light elements abundances, expansion rate, CMB spectrum, structure characteristics of the Universe, etc., it is possible to constrain the parameters of new physics (like neutrino oscillations).

Standard Big Bang Nucleosynthesis

During the early hot and dense epoch of the Universe ($T \leq 1$ MeV) D, ^{3}He, ^{4}He, ^{7}Li were synthesized successfully.

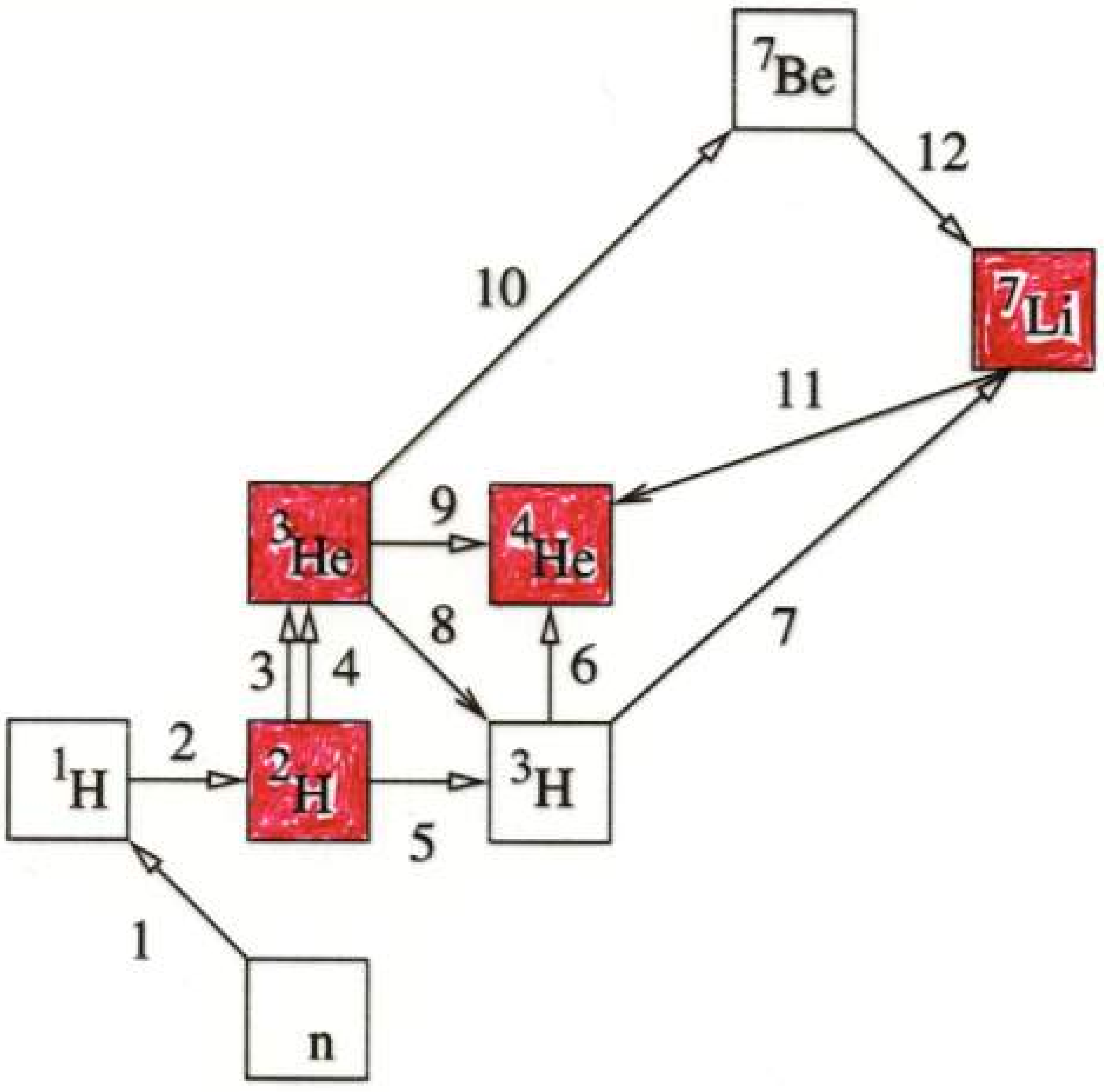

1. $p \longleftrightarrow n$
2. $p(n,\gamma)d$
3. $d(p,\gamma)^3$He
4. $d(d,n)^3$He
5. $d(d,p)t$
6. $t(d,n)^4$He
7. $t(\alpha,\gamma)^7$Li
8. ^{3}He$(n,p)t$
9. ^{3}He$(d,p)^4$He
10. ^{3}He$(\alpha,\gamma)^7$Be
11. ^{7}Li$(p,\alpha)^4$He
12. ^{7}Be$(n,p)^7$Li

^{4}He was the most abundantly produced - almost all available neutrons were bound into it.
Negligible amounts of D, ^{3}He and ^{7}Li were formed:

$$2 \times 10^{-5} \leq D/H \leq 5 \times 10^{-5}$$
$$10^{-5} \leq He^3/H \leq 5\,10^{-5}$$
$$1 \times 10^{-10} \leq Li^7/H \leq 4 \times 10^{-10}$$

Because of the low density, growing Coulomn barriers and stability gaps at A=5, A=8, the formation of larger nuclei was postponed until the formation of stars several billion years later.

SBBN assumes three neutrino flavours, zero lepton asymmetry and equilibrium neutrino number densities and spectrum:

$$n_\nu^{eq} = \exp(-E/T)/(1 + \exp(-E/T))$$

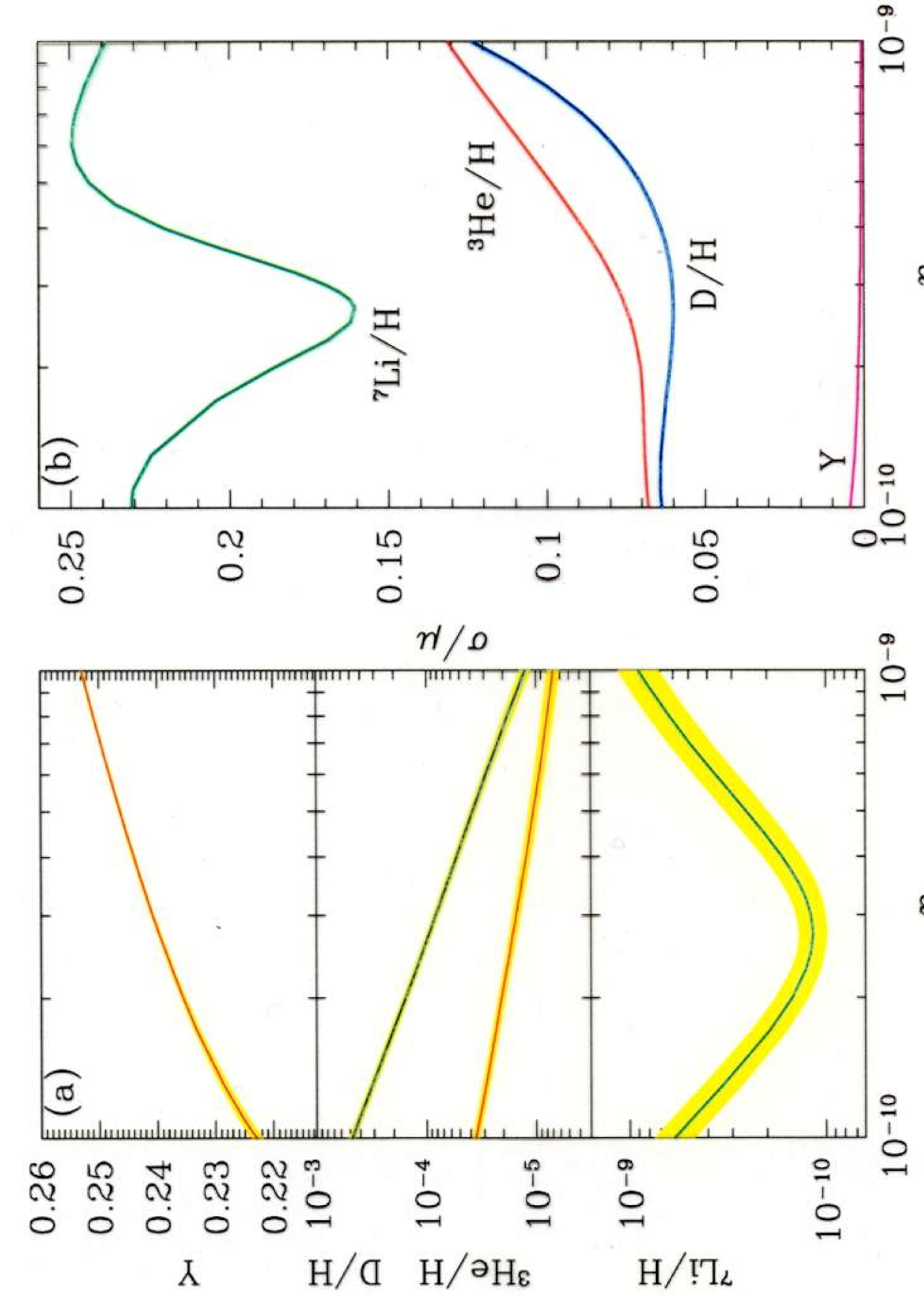

Fig. 6.— Light element abundance predictions, and their uncertainties, as a function of η. a) The solid curves are the (renormalized) NACRE abundance predictions, and the broken curves are the 1σ Monte Carlo errors for the NACRE high/low error estimates. b) The fractional errors in the light element predictions, for the NACRE high/low estimates as in (a) (solid curves). The fractional errors plotted are σ_i/μ_i, where μ_i is the mean value of abundance i, and σ_i is its error.

CFO astro-ph/0102179

The predicted abundances are in accordance with the observational data for the light elements (at the value of η obtained from deuterium measurements $\eta = 5 \times 10^{-10}$).

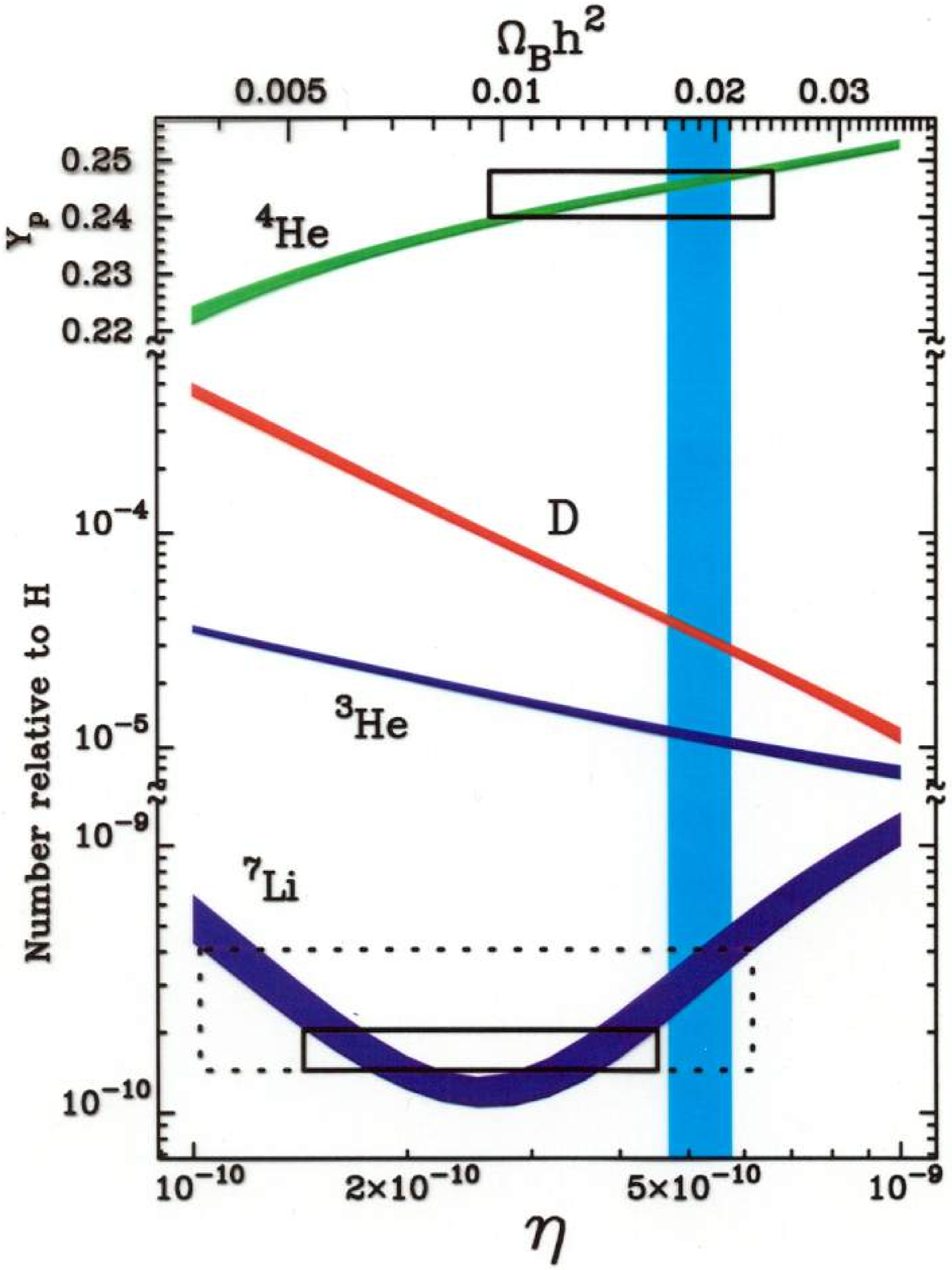

The dependence of the primordially produced elements on baryon-to-photon ratio η.

The thickness of the curves corresponds to 2σ theor. errors

$\Omega_B h^2 = 0.019 \pm 0.002$ (95% C.L)

for $D/H = 3.3 \pm 0.5 \cdot 10^{-5}$

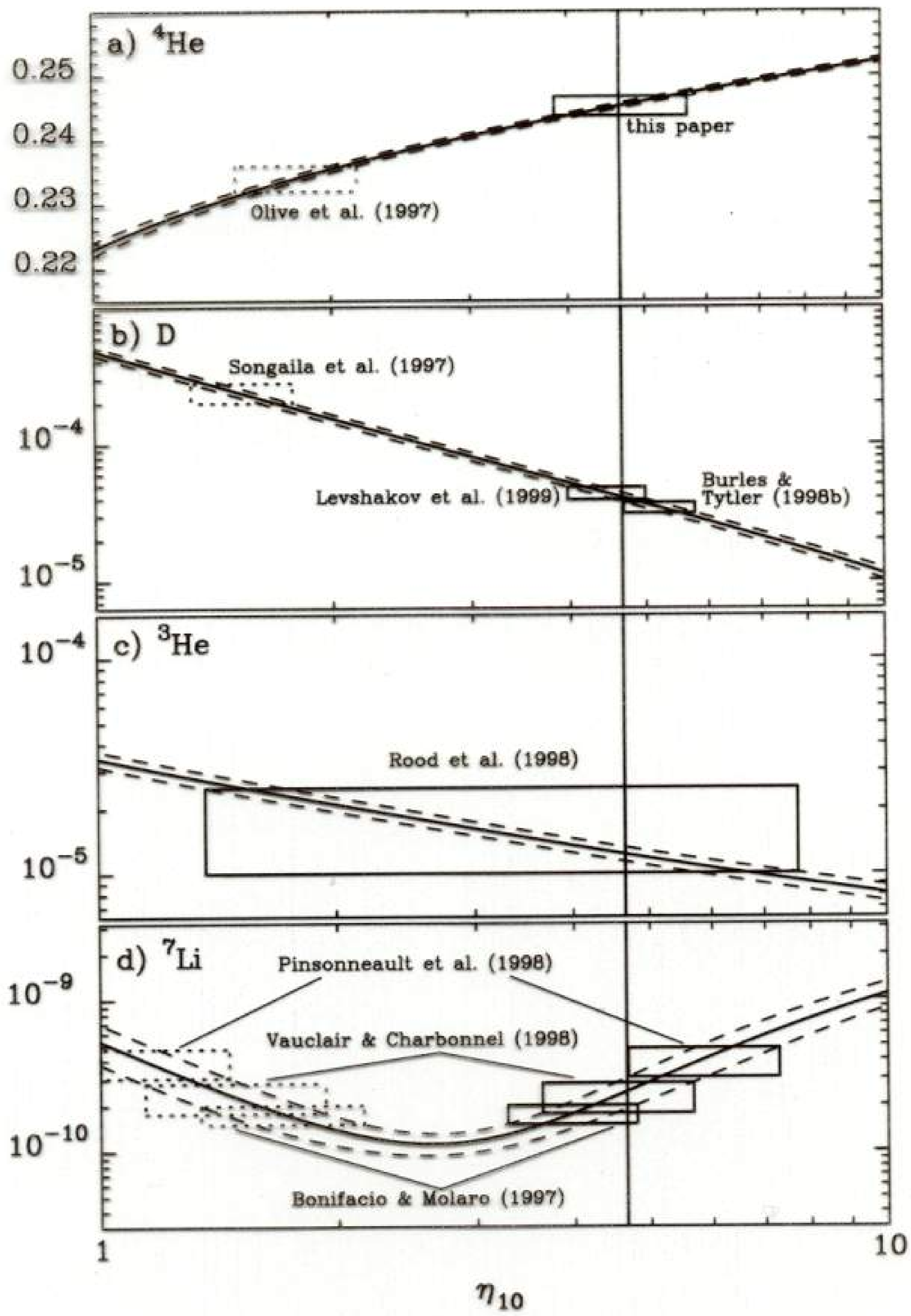

The abundance of (a) ^{4}He, (b) D, (c) ^{3}He and (d) ^{7}Li as a function of $\eta_{10} \equiv 10^{10}\ \eta$, where η is the baryon-to-photon number ratio, as given by the standard hot big bang nucleosynthesis model. The abundances of D, ^{3}He and ^{7}Li are number ratios relative to H. For ^{4}He, the mass fraction Y is shown. The value of Izotov & Thuan (1998) and Izotov et al. (1999) $Y_{\rm p} = 0.245 \pm 0.002$ gives $\eta = (4.7^{+1.0}_{-0.8}) \times 10^{-10}$ as shown by the solid vertical line. We show other data with 1σ boxes.

For a precise analysis of the oscillations effect on CN, helium-4 is used as far as the most reliable and abundant data now available are for that element.

The primordial yield of ^{4}He essentially depends on the freezing of the reactions interconverting neutrons and protons :

$$\begin{aligned} \nu_e + n &\leftrightarrow p + e^- \\ e^+ + n &\leftrightarrow p + \tilde{\nu}_e. \end{aligned} \tag{1}$$

Their freeze-out occurs when

$$\Gamma_w \sim G_F^2 E_\nu^2 N_\nu \leq H(t) \sim \sqrt{g_{eff}}\ T^2$$

^{4}He is a strong function of g_{eff} and neutron mean lifetime τ_n. and a logarithmic function of η, due to the nuclear reactions dependence on nucleon densities:

$$Y_p(g_{eff}, \tau_n, \eta)$$

Actually, it depends also on the electron neutrino number density and spectrum, and on the neutrino-antineutrino asymmetry, which enter through Γ_w.

Almost all neutrons, present at the start of nuclear reactions, are sucked into ^{4}He. So,

$$Y_p \sim 2(n/p)_f/(1 + n/p)_f \exp(-t/\tau_n)$$

The primordial ^{4}He abundance Y_p, predicted from SBBN, is calculated with great precision: the theoretical uncertainty is less than 0.1% ($|\delta Y_p| < 0.0002$) within a wide range of η.

Lopez R. E., and Turner M. S., Phys. Rev.D 59, 103502 (1999)

Nollett K. M., and Burles S., Phys. Rev.D 61, 123505 (2000)

GREAT SYSTEMATIC ERRORS PERHAPS...

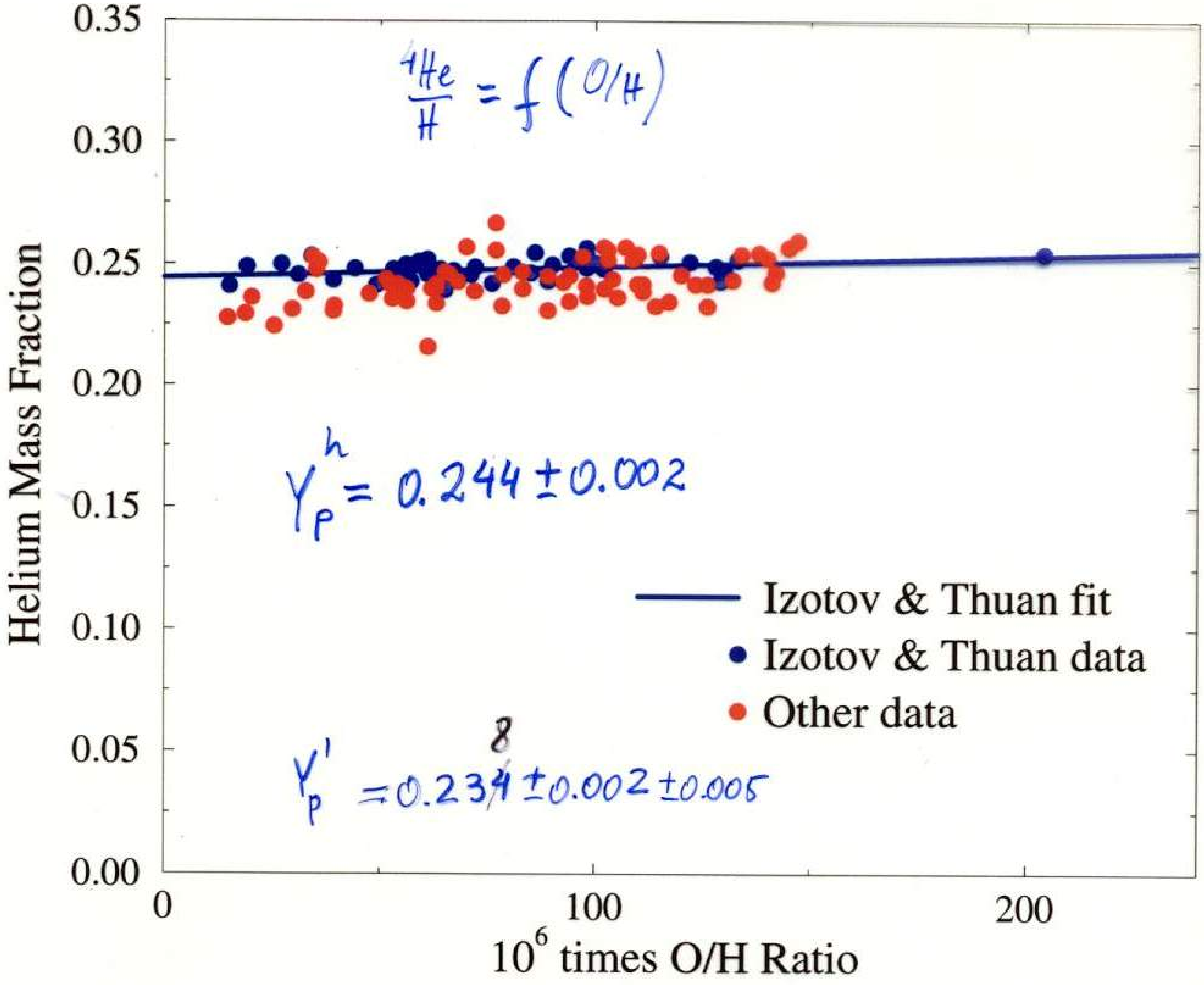

Y_p is inferred from measurements of $\frac{^4He}{H}$ in hot, ionized gas (H II regions) in other galaxies

Linear variation of He-4 abundance by mass with the metalicity Z is adopted: (Peimbert (74) Torres-Peimbert (76))

$$Y(Z) = Y_p + (\Delta Y / \Delta Z) Z + \Delta Y_s$$

pregalactic

$\frac{\Delta Y}{\Delta Z} \sim 2 \div 4$ helium to metals enrichment ratio

stellar contribution $\Delta Y_s = f(M_*)$

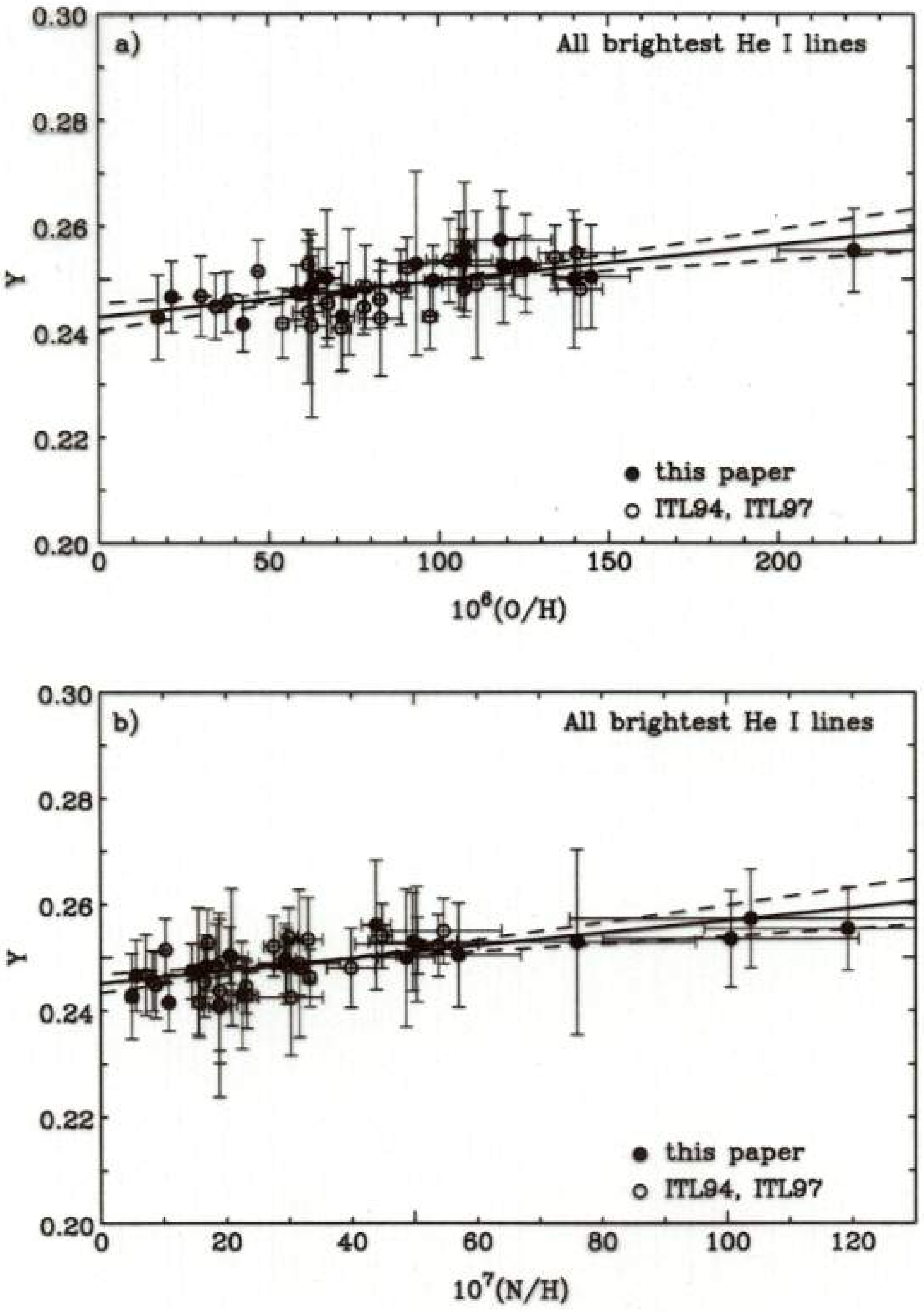

Linear regressions of (a) the helium mass fraction Y vs. oxygen abundance O/H and (b) the helium mass fraction Y vs. nitrogen abundance for our sample of 45 H II regions. The Ys are derived self-consistently by using the 5 brightest He I emission lines in the optical range. Collisional and fluorescent enhancements, underlying He I stellar absorption and Galactic Na I interstellar absorption are taken into account.

The predicted helium-4 value is in accordance with the contemporary helium values, inferred from observational data: 0.238–0.245 (the systematic errors are supposed to be around 0.007). The uncertainty of the observational Y_p is few percent.
Izotov Yu. I., and Thuan T. X.,Ap. J.500, 188 (1998)

Given this accuracy, it can be used as a probe of the eventual new neutrino physics — the neutrino oscillations.

Primordial Nucleosynthesis with Neutrino Oscillations

The presence of neutrino oscillations invalidates the main assumptions of BBN about three neutrino flavours, zero lepton asymmetry, equilibrium neutrino number densities and energy distribution, thus directly influencing the kinetics of nucleons during the weak freeze-out

The basic idea of oscillations is that mass eigenstates ν_i are distinct from the flavour eigenstates ν_f:

$$\nu_i = U_{if}\, \nu_f \qquad (f = e, \mu, \tau).$$

In the simple two-neutrino oscillation case, the probability to find at a distance l a given neutrino type in an initially homogeneous neutrino beam of the same type is:

$$P_{ff} = 1 - \sin^2 2\vartheta \sin^2\left(\frac{\delta m^2}{4E} l\right),$$

The medium distinguishes between different neutrino types due to their different interactions with fermions of the hot plasma at BBN epoch. This leads to different potentials for different neutrino types.

Matter oscillation parameters could be expressed through the vacuum ones and through the characteristics of the medium.

$$\sin^2 \vartheta_m = \sin^2 \vartheta / [\sin^2 \vartheta + (Q \mp L - \cos 2\vartheta)^2],$$

where $Q = -bE^2T^4/(\delta m^2 M_W^2)$, $L = -aET^3L^\alpha/(\delta m^2)$, L^α is expressed through the fermion asymmetries of the plasma, a and b are positive constants different for the different neutrino types. $-L$ corresponds to the neutrino and $+L$ to the antineutrino case.

In general the medium suppresses oscillations by decreasing their amplitude,

A possibility of enhanced oscillations transfer exists, in case a resonant condition holds:

$$Q \mp L = \cos 2\vartheta \qquad (2)$$

At BBN epoch with the cooling of the Universe, an interesting interplay between the two terms is observed:
At high temperatures: $|Q| > |L|$
$\delta m^2 > 0$ corresponds to a nonresonant case,
$\delta m^2 < 0$ corresponds to a resonant case.
The resonance holds in both neutrino and antineutrino sectors.

At low temperatures: $|Q| < |L|$
the resonance is possible for neutrinos if $\delta m^2 > 0$
or
for antineutrinos if $\delta m^2 < 0$.

Cosmological constraints on $\nu_{\mu,\tau} \leftrightarrow \nu_s$

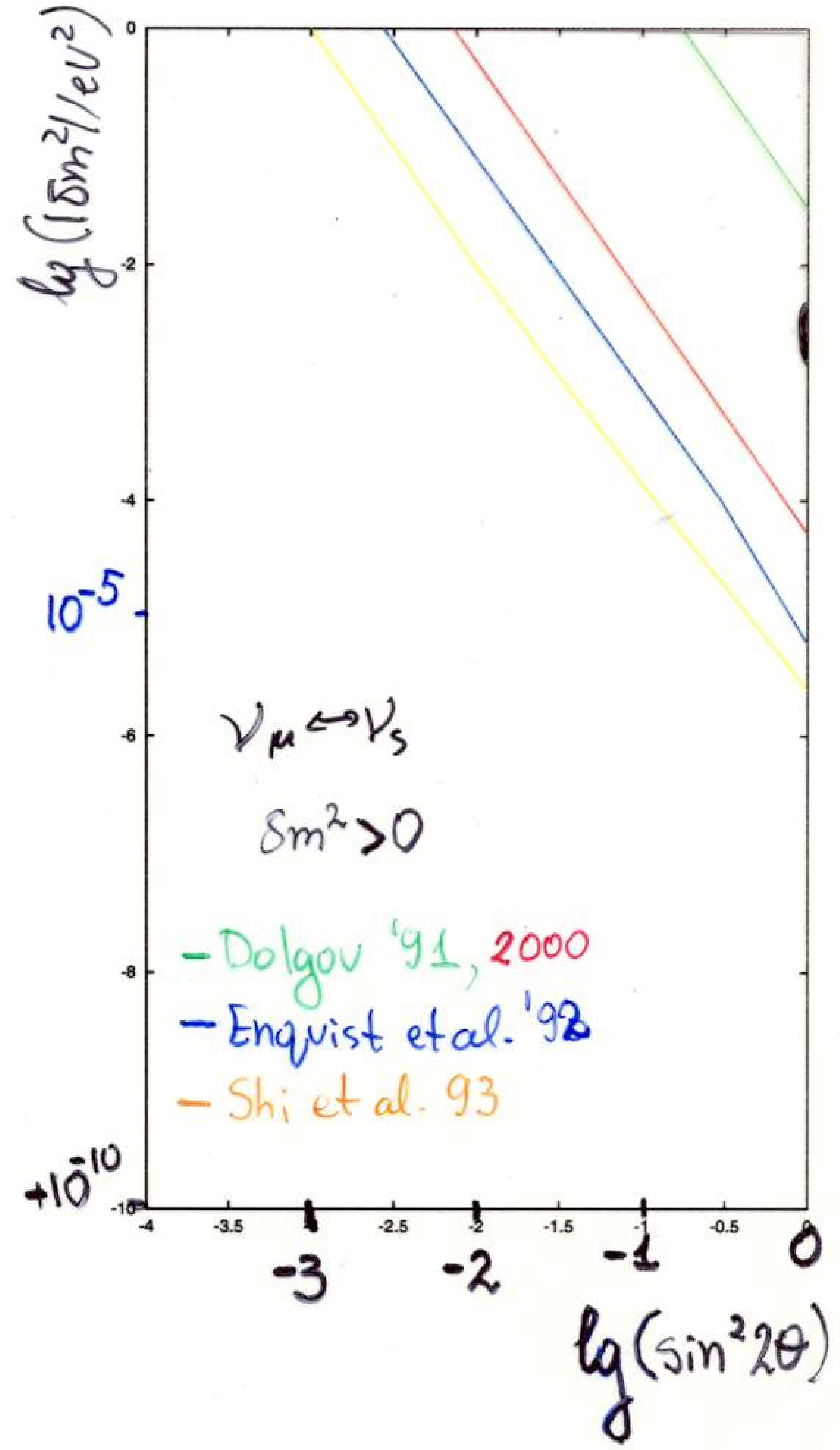

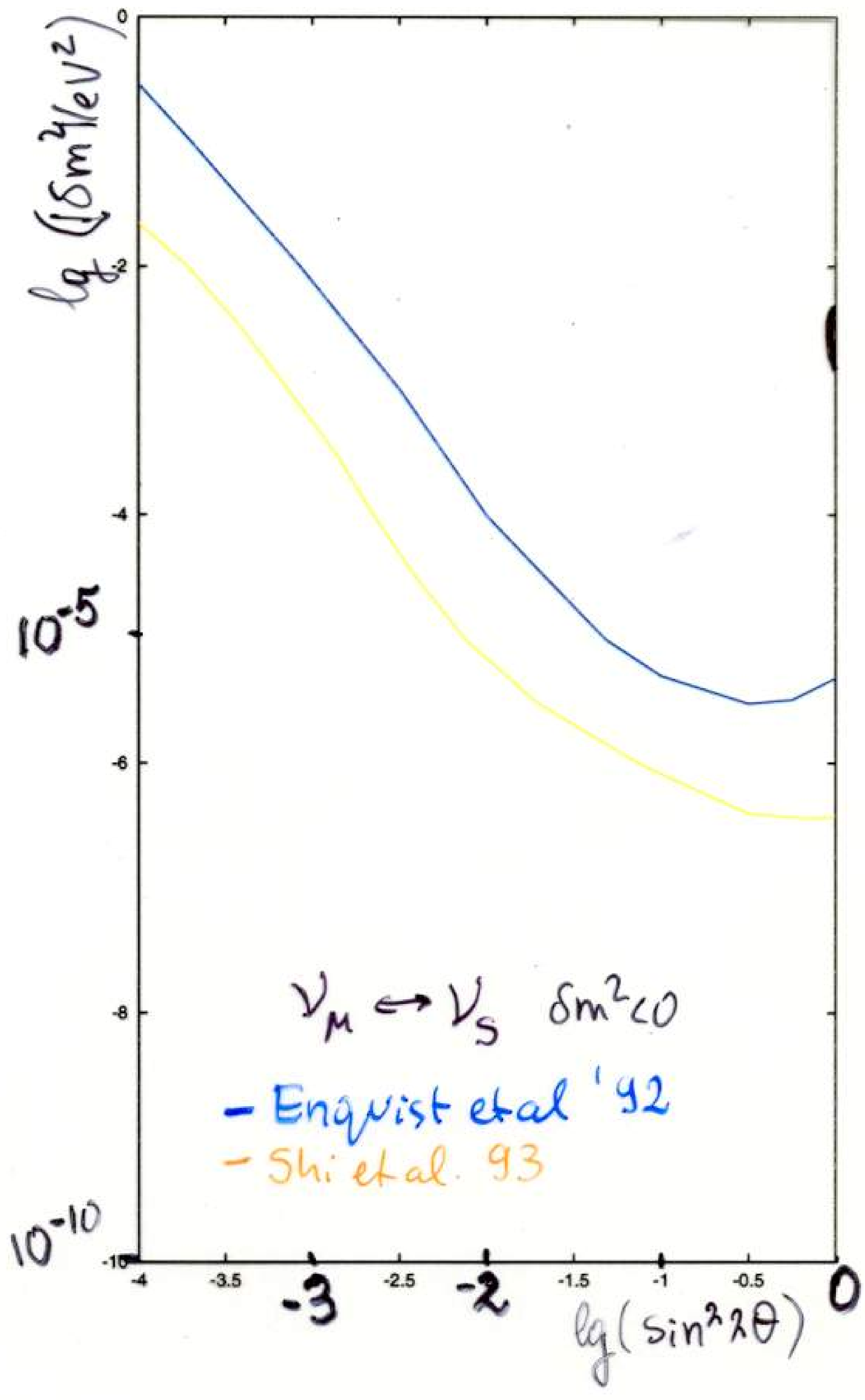

lg (|δm²|/eV²)
0
-2
-4
10^-5
-6
-8
10^-10
-10
-4
-3.5
-3
-2.5
-2
-1.5
-1
-0.5
0
lg(sin²2θ)
ν_μ ↔ ν_s δm²<0
- Enqvist et al '92
- Shi et al. 93

cosmological constraints on $\nu_e \leftrightarrow \nu_s$ (old ones)

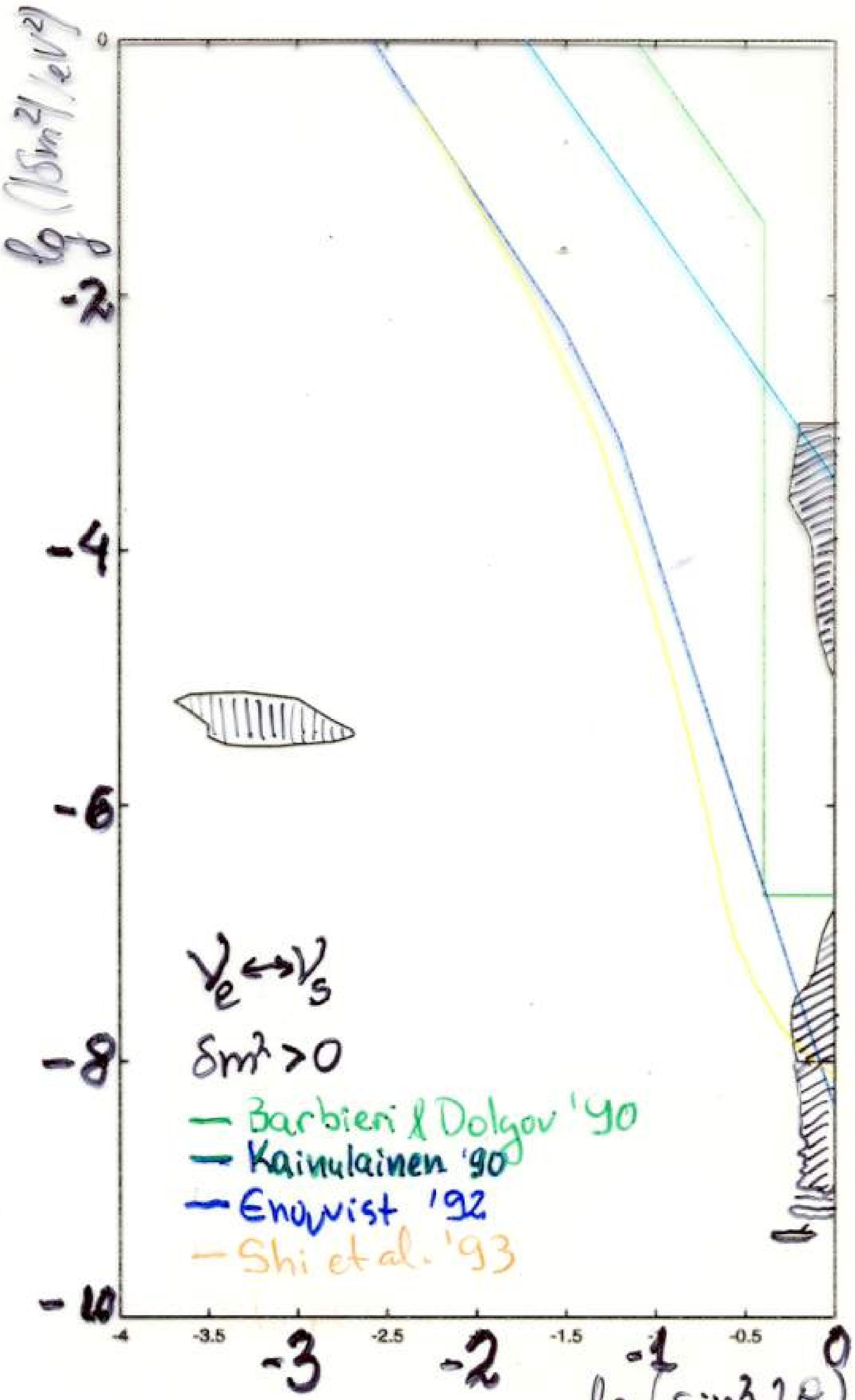

LOW, LMA from Suzuki, NOW 2000

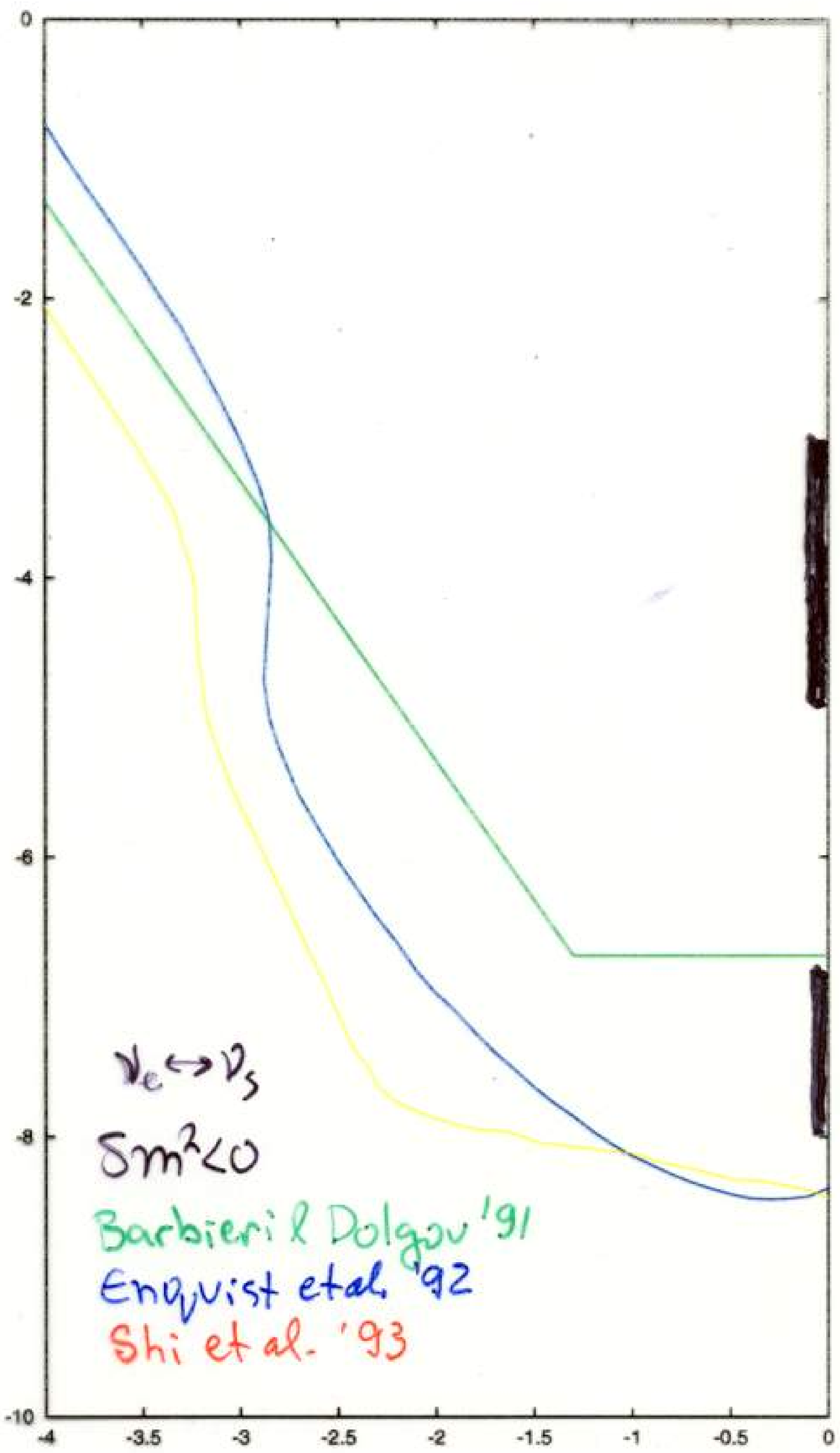
0
-2
-4
-6
-8
-10
-4
-3.5
-3
-2.5
-2
-1.5
-1
-0.5
0
$\nu_e \leftrightarrow \nu_s$
$\delta m^2 < 0$
Barbieri & Dolgov '91
Enqvist et al. '92
Shi et al. '93

Neutrino oscillations are capable to :

- bring additional degrees of freedom into equilibrium

This leads to faster Universe expansion $H(t) \sim g_{eff}^{1/2}$, earlier n/p-freezing, $T_f \sim (g_{eff})^{1/6}$, at times when neutrons were more abundant

$$n/p \sim \exp(-(m_n - m_p)/T_f)$$

and overproduction of helium-4.
Dolgov A.D., Sov. J. Nucl. Phys. 33, 700 (1981).

- deplete the neutrino number densities N_ν $N_\nu \neq N_\nu^{eq}$

Electron neutrino depletion slows down the weak rates, $\Gamma_w \sim N_\nu E_\nu^2$, and leads to an earlier n/p-freezing and overproduction of He-4 yield.
D.P.K, JINR E2-88-301, 1988

- distort the neutrino spectrum

Oscillation rate is energy dependent
$\Gamma_{osc} \sim \delta m^2/E_\nu$ hence, the spectrum of the neutrinos may become strongly distorted.
D. P. K., JINR E2-88-301, 1988
D.P.K., Chizhov M.V., Proc. NEUTRINO 96 Conference, Helsinki, 478 (1996).

- produce neutrino-antineutrino asymmetry $N_\nu \neq N_{\bar\nu}$

Neutrino-antineutrino asymmetry may be generated during the resonant transfer of neutrinos.
Miheev S., Smirnov A., in VI Moriond Meeting on Massive Neutrinos in Particle Physics and Astrophyisics, Tignes, p.355, 1986.
Langacker P., Petcov S., Steigman G., and Toshev S., Nucl. Phys.B 282, 589 (1987)
The effect of asymmetry on ^{4}He abundance was analyzed for hundreds of $\delta m^2 - \vartheta$ combinations in *D.P.K., and Chizhov M. V., Nucl. Phys.B 591, 457 (2000); astro-ph/0101083.*

$$\frac{\partial N_n}{\partial t} = -3HN_n - N_\nu N_n \Gamma_w(\nu n \to pe^-) + N_p N_{\bar\nu}\Gamma(p\bar\nu \to e^+ n) + N_p N_e \Gamma(pe \to \nu n) - N_{e^+} N_n \Gamma(ne^+ \to p\bar\nu)$$

The evolution of energy distorsion of ν_e $x^2\rho_{LL}(x)$, where $x = E/T$

The dashed line corresponds to the equilibrium distribution at the same temperature.

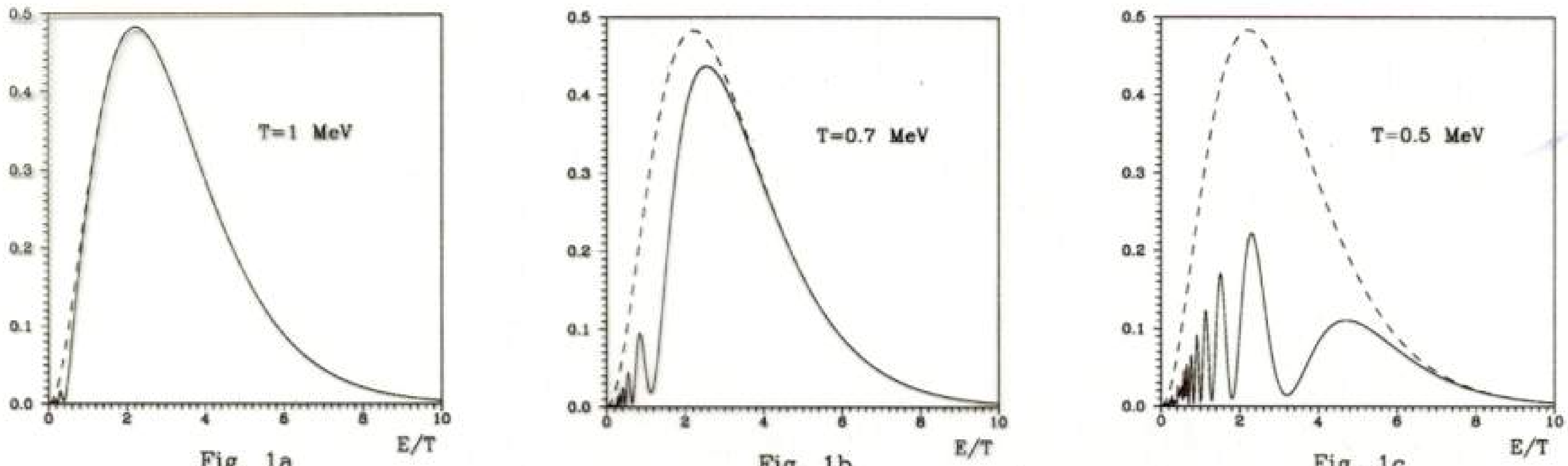

Fig. 1a Fig. 1b Fig. 1c

resonant case, $\delta m^2 = -10^{-8}\,eV^2$, $\theta = \frac{\pi}{8}$

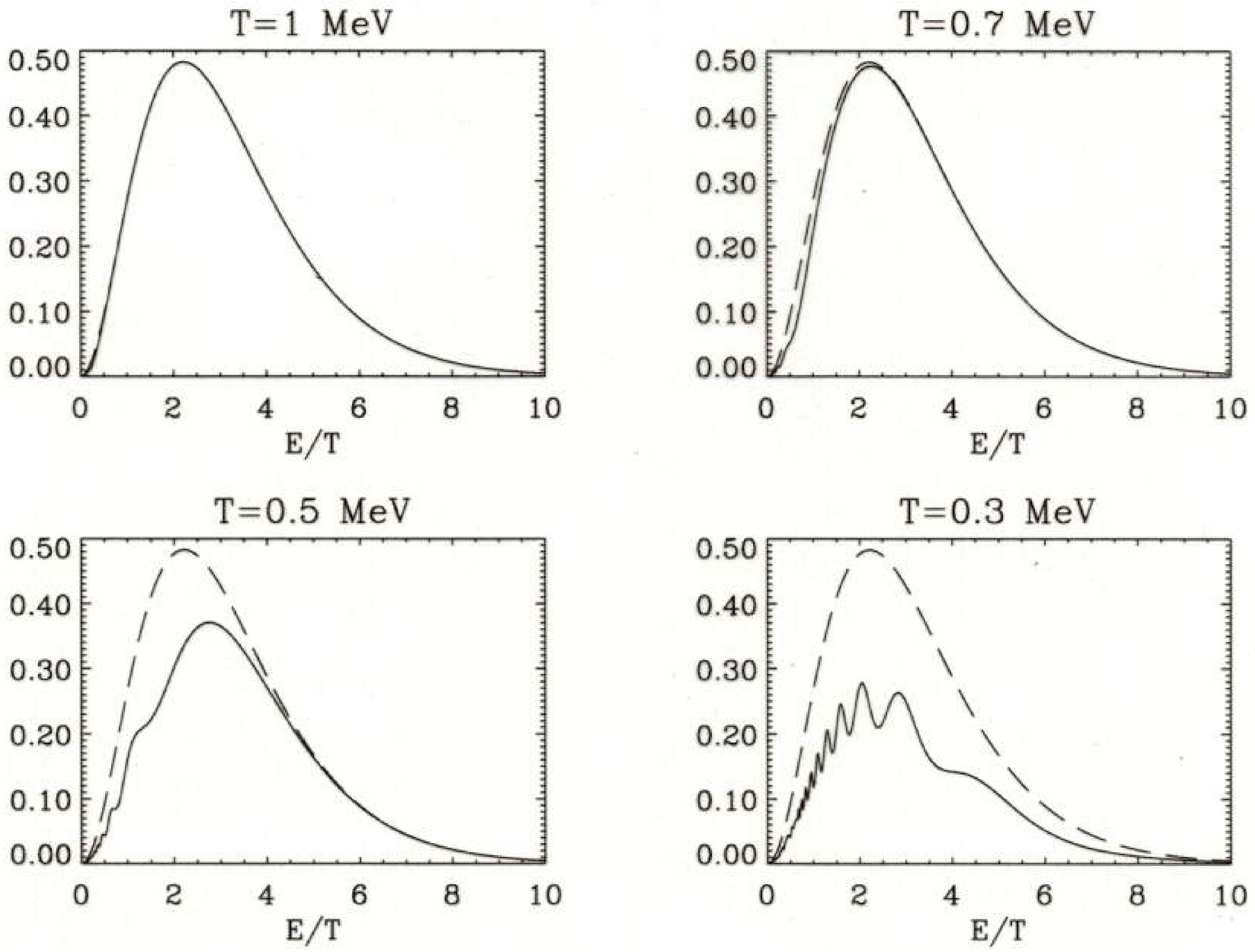

nonresonant case

The net effect of spectrum distortion on the production of He-4 due to neutrino oscillations

The distortion has two aspects:
a decrease of the energy leads to a decrease Γ_w, and increases the freezing temperature and He-4.

On the other hand, due to the threshold for the reaction $\tilde{\nu}_e + p \rightarrow n + e^+$ when the energy of the neutrinos becomes smaller than that threshold, the $(n/p)_F$-ratio decreases leading to a decrease of He.
The total effect is overproduction of He-4.

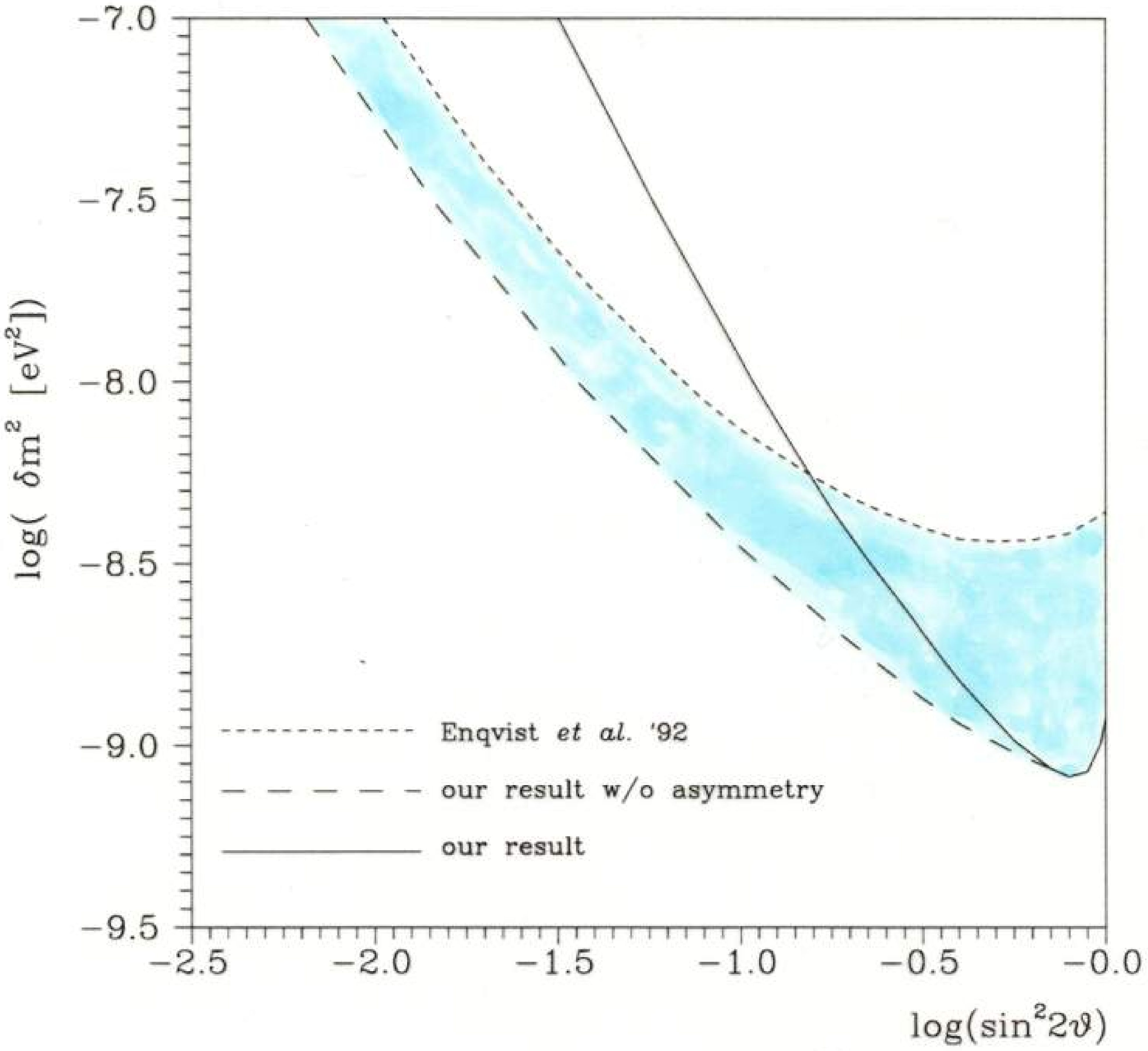

The effect is given by the region between the dotted curve (calculated without the account of the effect) and the dashed one.
D.P.K., Chizhov M.V., Nucl.Phys.B 591,457(2000).

Dynamically produced asymmetry suppresses oscillations at small mixing angles, leading to less overproduction of He-4.

Dynamically produced asymmetry exerts back effect to oscillating neutrino and may change its oscillation pattern. Thus it may effect indirectly BBN, even when its value is not high enough to have a direct kinetic effect on the synthesis of light elements: $L \ll 0.01$
D.P.K., Chizhov M.V., Proc. NEUTRINO 96 Conference, Helsinki, 478 (1996).

Even very small asymmetries $L \ll 0.01$ considerably influence nucleosynthesis through oscillations, hence asymmetry effect on nucleosynthesis should be accounted for during asymmetry's full evolution.

In the resonant case the asymmetry effect on BBN is considerable – up to about 10% relative decrease in He-4.

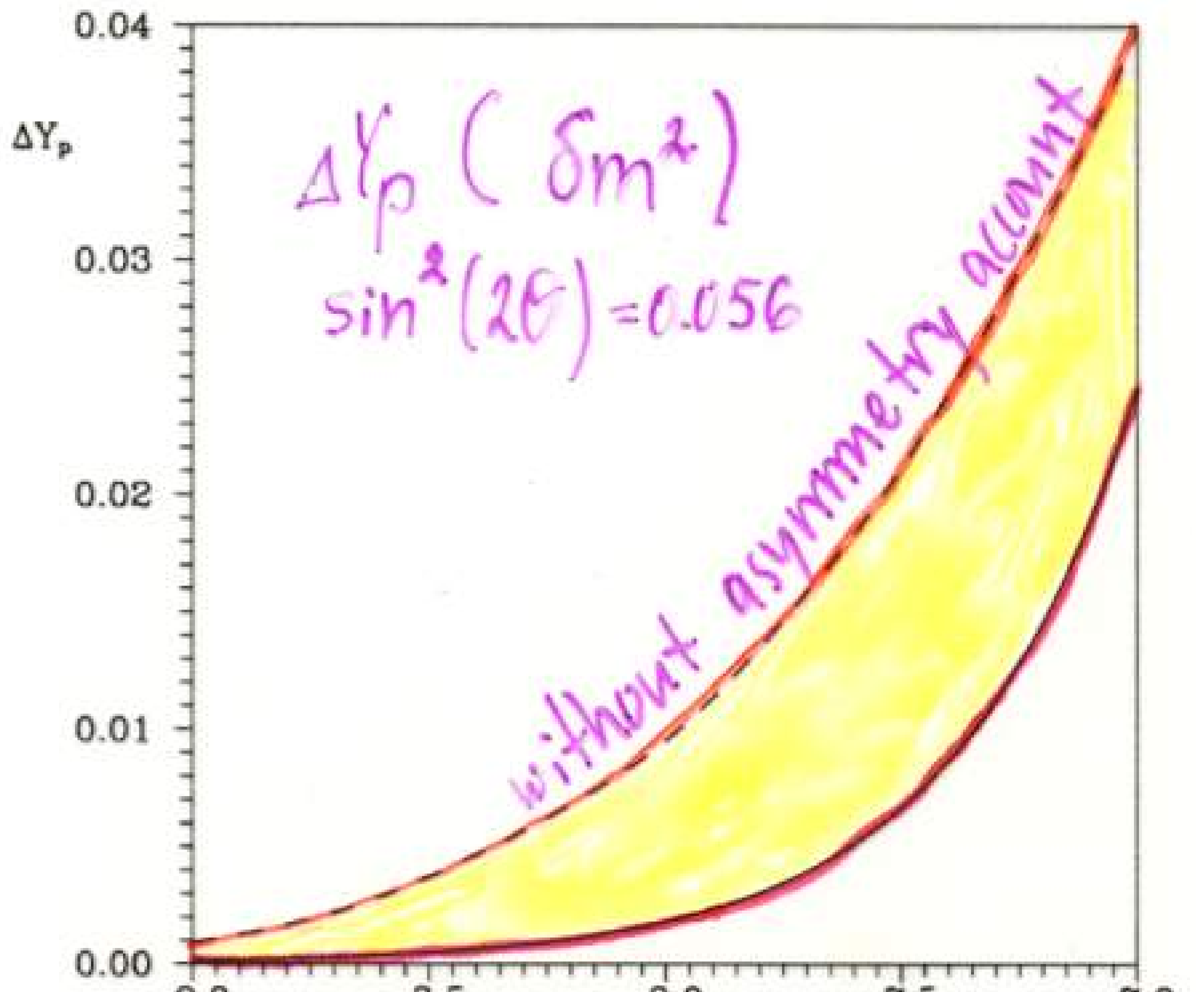

Relative change in the primordial He-4 production as a function of δm^2
— complete oscillations effect
— neglecting dynamical asymmetry

Dynamically produced asymmetry suppresses oscillations at small mixing angles, leading to less overproduction of He-4.

The effect of the oscillations generated asymmetry on He-4

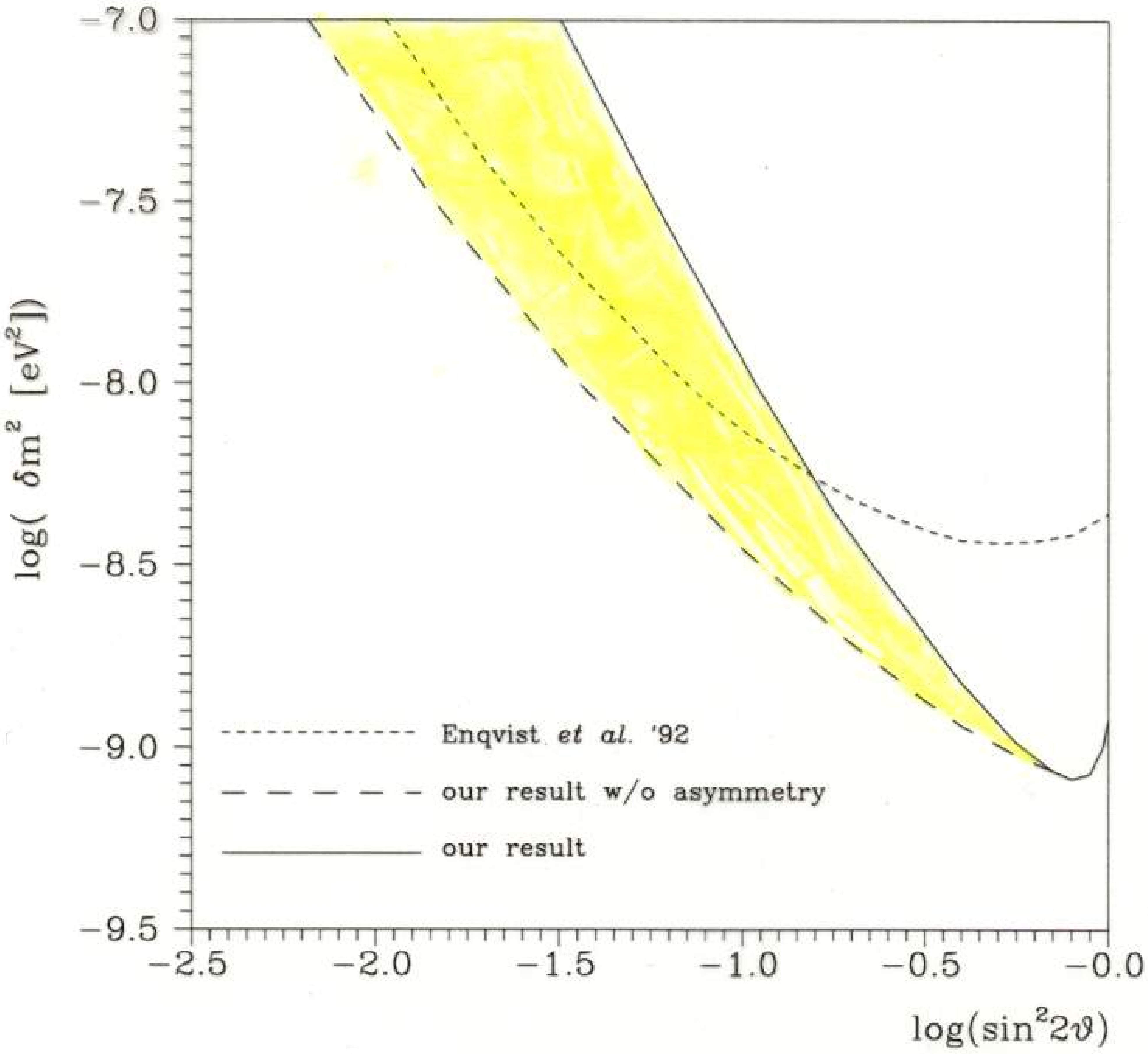

The net asymmetry effect is given by the region between the dashed (without asymmetry account) and the solid curves.

D.P.K., Chizhov M.V., Nucl.Phys.B 591,457(2000).

The kinetics

A selfconsistent numerical analysis of the kinetics of the oscil-lating
neutrinos, the nucleons freeze-out and the asymmetry evolution was provided.

expansion

$$\partial\rho(t)/\partial t = Hp_\nu \ (\partial\rho(t)/\partial p_\nu) + $$
$$+i\,[\mathcal{H}_o,\rho(t)] + i\sqrt{2}G_F\left(\mathcal{L} - Q/M_W^2\right)N_\gamma\,[\alpha,\rho(t)] + \mathrm{O}\left(G_F^2\right),$$

oscillations medium forward collisions second order medium effects

$$\partial\bar\rho(t)/\partial t = Hp_\nu \ (\partial\bar\rho(t)/\partial p_\nu) + $$
$$+\ \mathrm{i}\ [\mathcal{H}_o,\bar\rho(t)] + i\sqrt{2}G_F\left(-\mathcal{L} - Q/M_W^2\right)N_\gamma\,[\alpha,\bar\rho(t)] + \mathrm{O}\left(G_F^2\right),$$

$$\partial n_n/\partial t = Hp_n \ (\partial n_n/\partial p_n) + $$
$$+ \int \mathrm{d}\Omega(e^-,p,\nu)|\mathcal{A}(e^-p\to\nu n)|^2\,[n_{e^-}n_p(1-\rho_{LL}) - n_n\rho_{LL}(1-n_{e^-})]$$
$$- \int \mathrm{d}\Omega(e^+,p,\tilde\nu)|\mathcal{A}(e^+n\to p\tilde\nu)|^2\,[n_{e^+}n_n(1-\bar\rho_{LL}) - n_p\bar\rho_{LL}(1-n_{e^+})].$$

$\alpha_{ij} = U^*_{ie}U_{je}$, $\nu_i = U_{il}\nu_l (l = e, s)$.
$\mathcal{H}_o$ **is the free neutrino Hamiltonian.**
Q **arises as an** W/Z **propagator effect,** $Q \sim E_\nu\, T$.
$\mathcal{L} \sim 2L_{\nu_e} + L_{\nu_\mu} + L_{\nu_\tau}$, $L_{\mu,\tau} \sim (N_{\mu,\tau} - N_{\bar\mu,\bar\tau})/N_\gamma$
$L_{\nu_e} \sim \int \mathrm{d}^3p(\rho_{LL} - \bar\rho_{LL})/N_\gamma$.
$\rho_{LL} = c^2\rho_{11} - sc\,(\rho_{12}+\rho_{21}) + s^2\rho_{22}$ $\quad n_{\nu_e}(p,t) = \rho_{LL}(p,t)$

Kinetic equations for neutrino density matrix and neutron number densities in *momentum space* **were used to describe oscillating neutrinos in the high temperature Universe. This allows precise account for spectrum distortion effect, neutrino depletion and neutrino asymmetry and its back effect at each neutrino momentum.**

The equations provide a *simultaneous account* **of the different competing processes: expansion, neutrino oscillations and weak interaction processes.**

The numerical analysis was provided for the temperature interval [0.3 MeV, 2 MeV]

The last term describes the weak interactions of neutrinos with the medium:

$e^+e^- \leftrightarrow \nu_i\tilde{\nu}_j$

$e^\pm\nu_j \rightarrow e'^\pm\nu'_i$

$$\begin{aligned} & \int d\Omega(\tilde{\nu}, e^+, e^-)\left[n_{e^-}n_{e^+}\mathcal{A}\mathcal{A}^\dagger - \tfrac{1}{2}\left\{\rho,\ \mathcal{A}^\dagger\bar{\rho}\mathcal{A}\right\}_+\right] \\ + & \int d\Omega(e^-, \nu', e'^-)\left[n'_{e^-}\mathcal{B}\rho'\mathcal{B}^\dagger - \tfrac{1}{2}\left\{\mathcal{B}^\dagger\mathcal{B},\ \rho\right\}_+ n_{e^-}\right] \\ + & \int d\Omega(e^+, \nu', e'^+)\left[n'_{e^+}\mathcal{C}\rho'\mathcal{C}^\dagger - \tfrac{1}{2}\left\{\mathcal{C}^\dagger\mathcal{C},\ \rho\right\}_+ n_{e^+}\right], \end{aligned}$$

$\mathcal{A}$ is the amplitude of $e^+e^- \rightarrow \nu_i\tilde{\nu}_j$, $\mathcal{B}$ is the amplitude of $e^-\nu_j \rightarrow e'^-\nu'_i$ and $\mathcal{C}$ is the amplitude of $e^+\nu_j \rightarrow e'^+\nu'_i$.

$$\mathcal{A} = \alpha\,\mathcal{A}_e, \qquad \mathcal{B} = \alpha\,\mathcal{B}_e, \qquad \mathcal{C} = \alpha\,\mathcal{C}_e.$$

$\mathcal{A}_e(e^+e^- \rightarrow \nu_e\tilde{\nu}_e)$, $\mathcal{B}_e(e^-\nu_e \rightarrow e^-\nu_e)$, $C_e(e^+\nu_e \rightarrow e^+\nu_e)$

$T \geq 2\ MeV$ $\quad n_\nu(p) = n_\nu^{eq}(-p/T) \doteq \frac{e^{-p/T}}{1+e^{-p/T}}$ $\quad \rho^0_{2MeV} = \begin{pmatrix} c^2 & -cs \\ -cs & s^2 \end{pmatrix} n_\nu^{eq}$

Neutrino kinetics down to 2 MeV is the standard one, i.e. electron neutrinos maintain their equilibrium distribution, while sterile neutrinos are absent.

The equation results into a set of coupled nonlinear integro-differential equations for the components of the density matrix of neutrino.

- Neutrino and antineutrino ensembles $\overbrace{\text{evolve}}^{\text{may}}$ differently as far as the background is not CP symmetric. $\rho_\nu(t) \neq \rho_{\bar{\nu}}(t)$

- Oscillations change neutrino-antineutrino asymmetry and it in turn affects oscillations. The evolution of neutrino and antineutrino ensembles becomes coupled and the evolution of neutrinos and antineutrinos must be considered simultaneously.

$$\frac{\partial\rho_\nu}{\partial t} = f_\nu\left(\rho_\nu,\ \rho_\nu - \rho_{\bar{\nu}},\ \rho_\nu + \rho_{\bar{\nu}}\right)$$

$$\frac{\partial\rho_{\bar{\nu}}}{\partial t} = f_{\bar{\nu}}\left(\rho_{\bar{\nu}},\ \rho_\nu - \rho_{\bar{\nu}},\ \rho_\nu + \rho_{\bar{\nu}}\right)$$

He-4 overproduction due to neutrino oscillations

In the nonresonance case **oscillations effect becomes very small (less than 1%) for small mixings: as small as $sin^2 2\vartheta = 0.1$ for $\delta m^2 = 10^{-7} eV^2$,**
and for small mass differences: $\delta m^2 < 10^{-10} eV^2$ at maximal mixing.
For $\delta m^2 \leq 10^{-11}$ eV^2, or at $\sin^2 2\vartheta \leq 10^{-3}$, the effect on nucleosynthesis is negligible.
The effect of oscillations is maximal at maximal mixing and greatest mass differences.

The dependence of the frozen neutron number density on the mixing angle (nonresonant case):

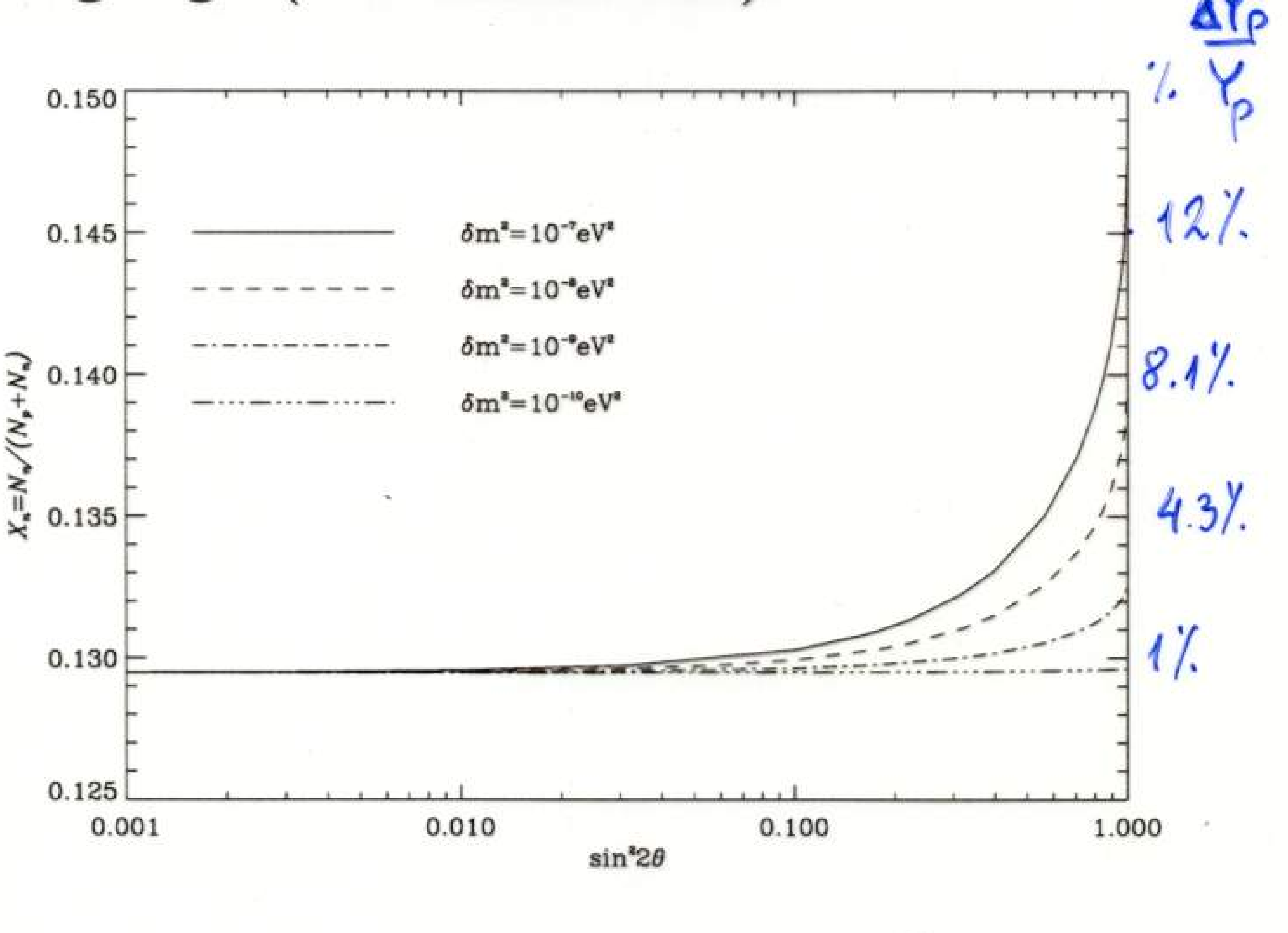

The primordially produced helium-4 Y_p as a function of neutrino mass differences at maximal mixing:

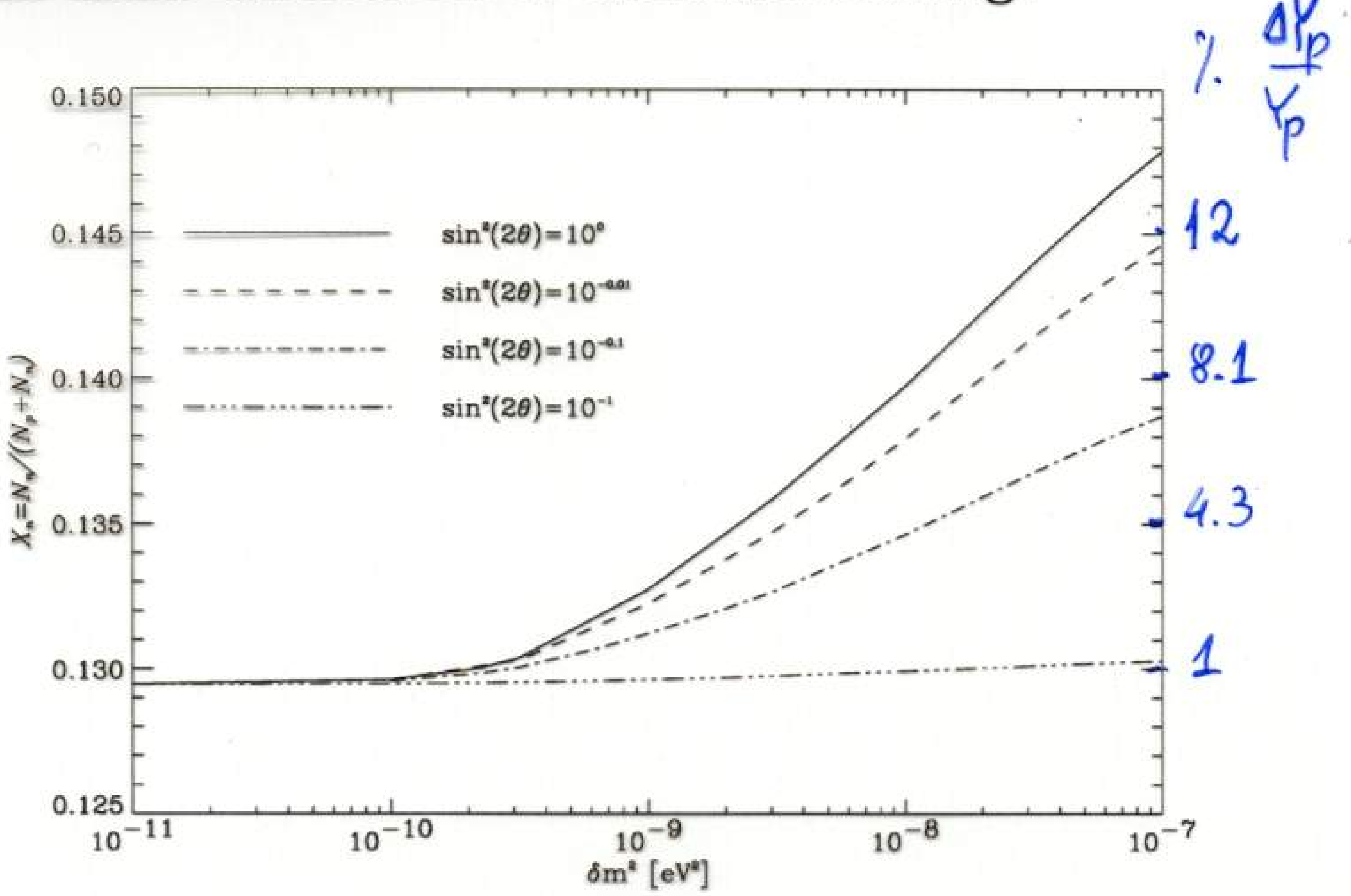

In the resonant case for a given δm^2 there exists a resonant mixing angle, at which the oscillations are enhanced by the medium, and hence, the overproduction of ^{4}He is greater than that corresponding to the vacuum maximal mixing angle.

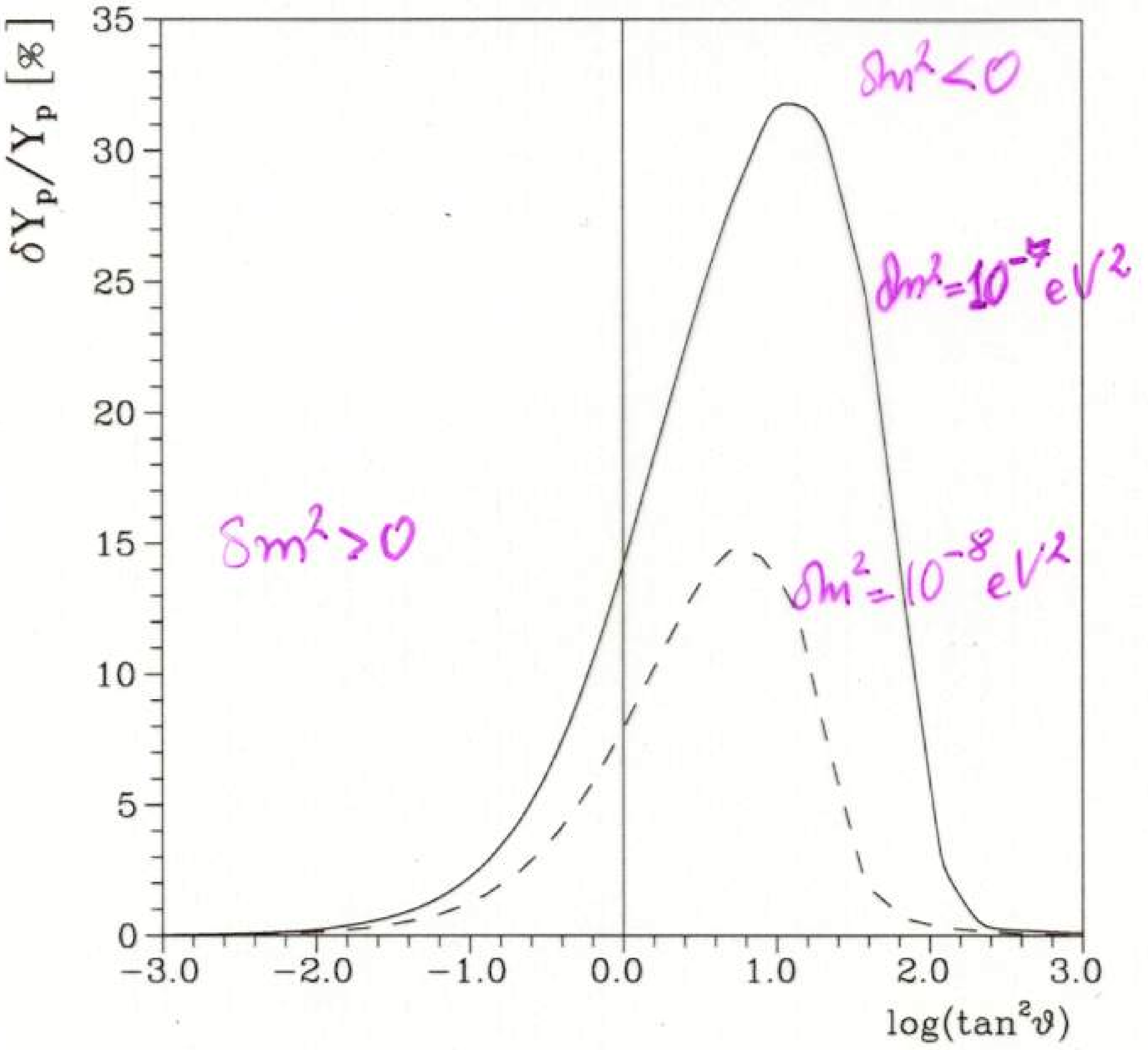

A combined plot for the resonant and the nonresonant oscillation case of δY_p as a function of the mixing angle for $\delta m^2 = 10^{-7}$ eV^2 and $\delta m^2 = 10^{-8}$ eV^2.

The maximal relative increase in the primordially produced ^{4}He $\delta Y_p^{max}/Y_p = (Y_{osc}^{max} - Y_p)/Y_p = f(\delta m^2)$ as a function of neutrino mass differences at maximal mixing for the nonresonant case and at the resonant mixing angle for the resonant case (upper curve).

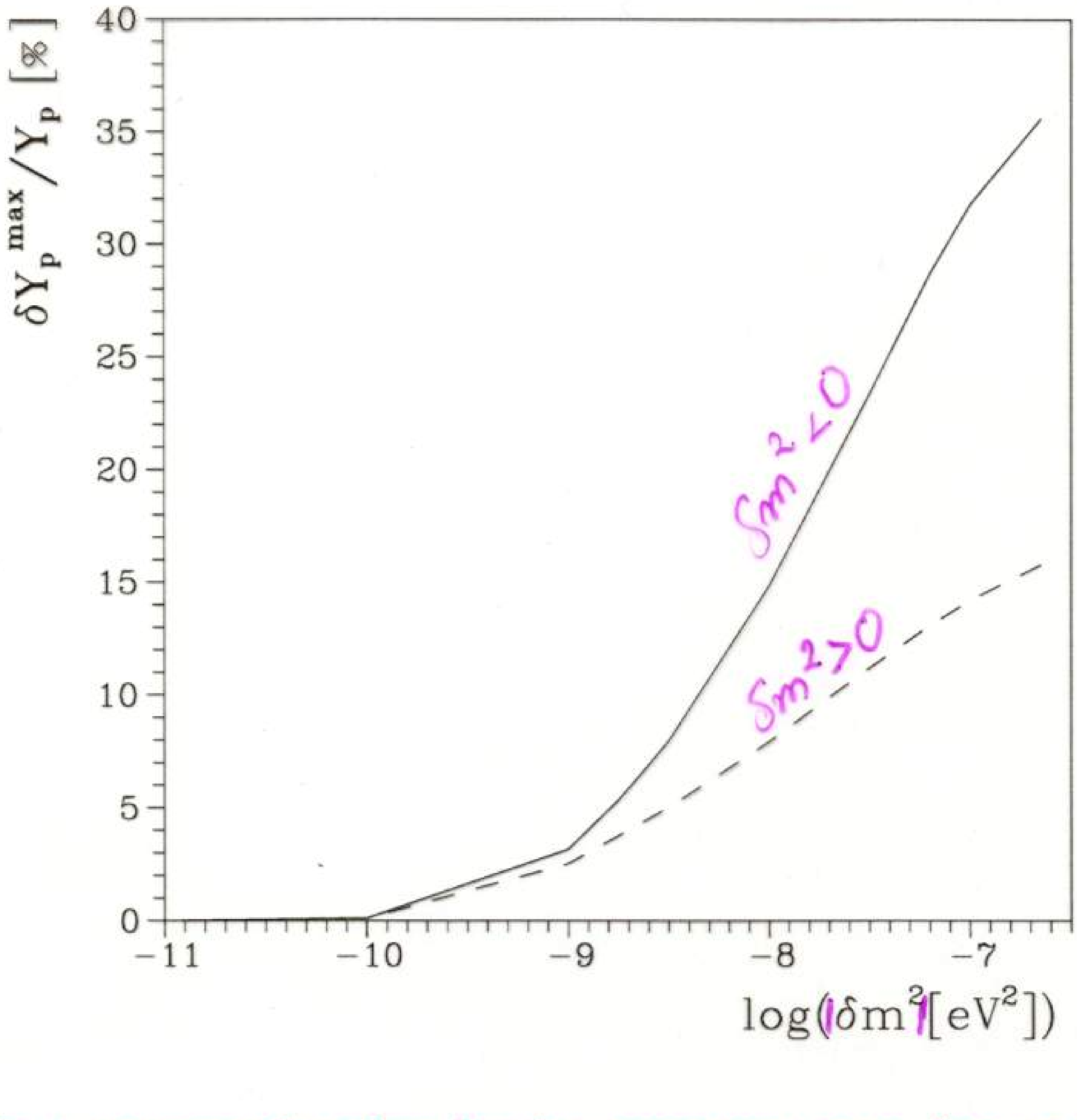

He-4 overproduction in the resonant case (up to 34%) is much greater than in the nonresonant one (up to 14%).

SOME ISOHELIUM CONTOURS

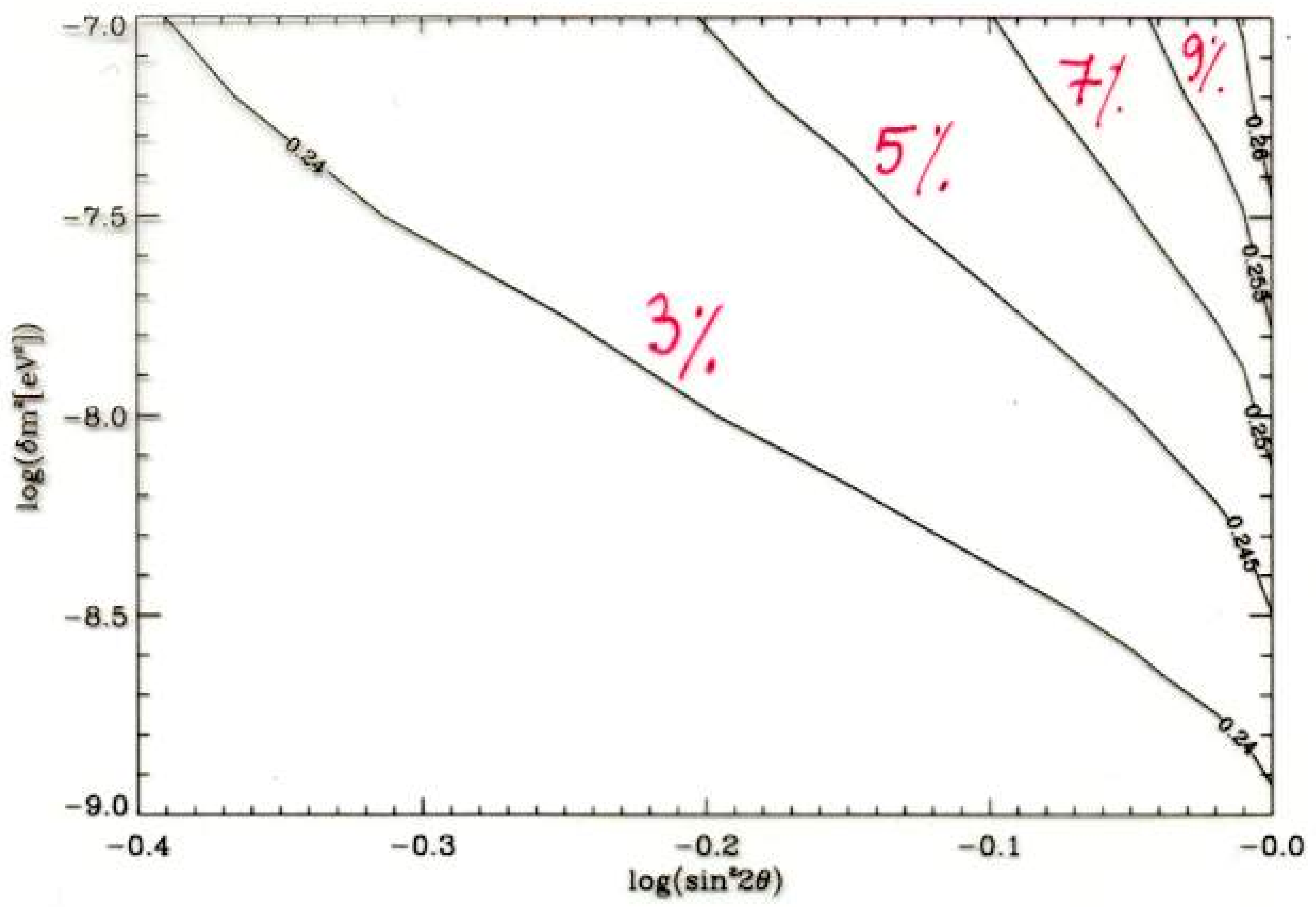

nonresonant case

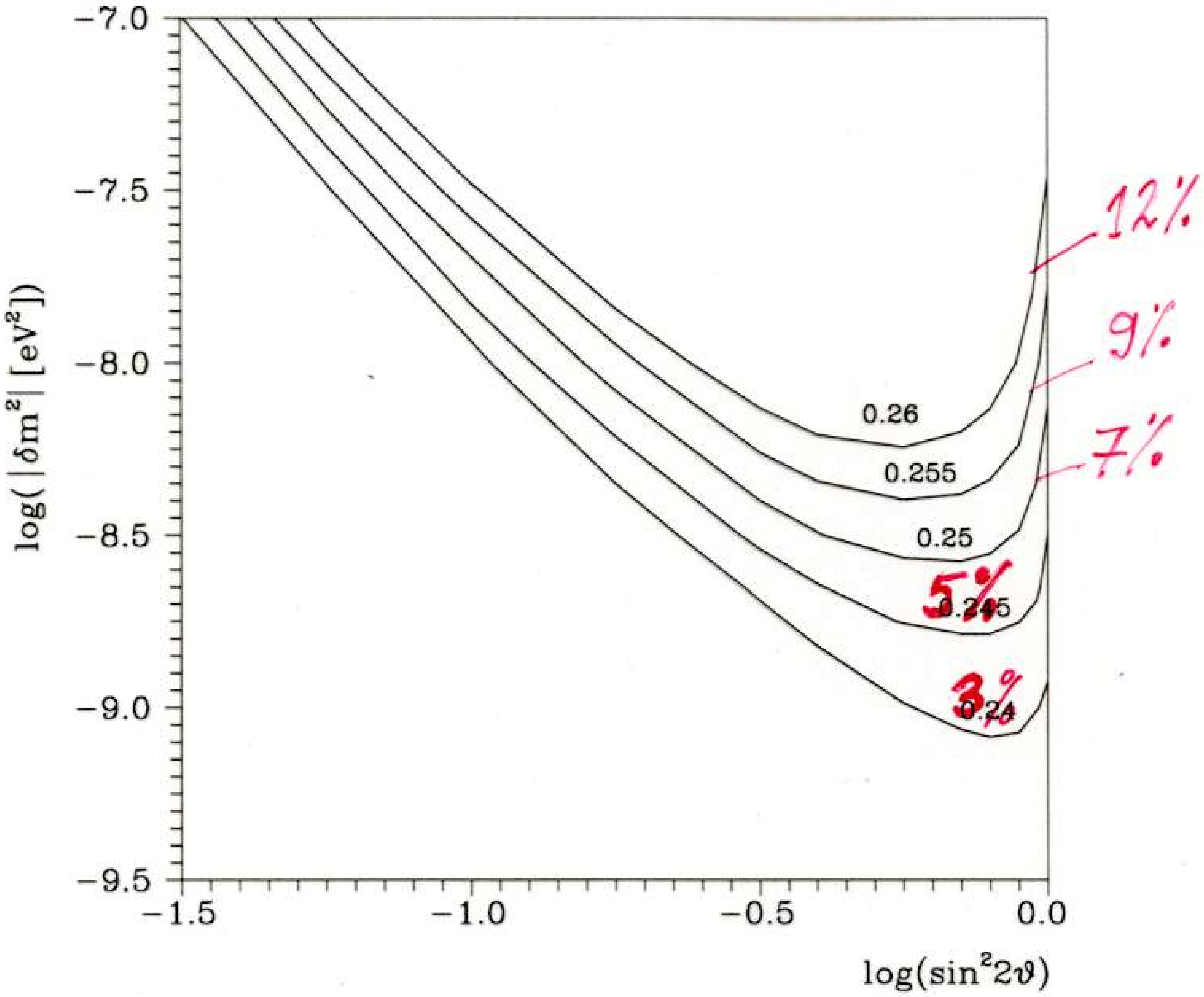

resonant case

Cosmological constraints on oscillation parameters

Observational data on primordial ^{4}He abundance put stringent limits on the allowed oscillation parameters.

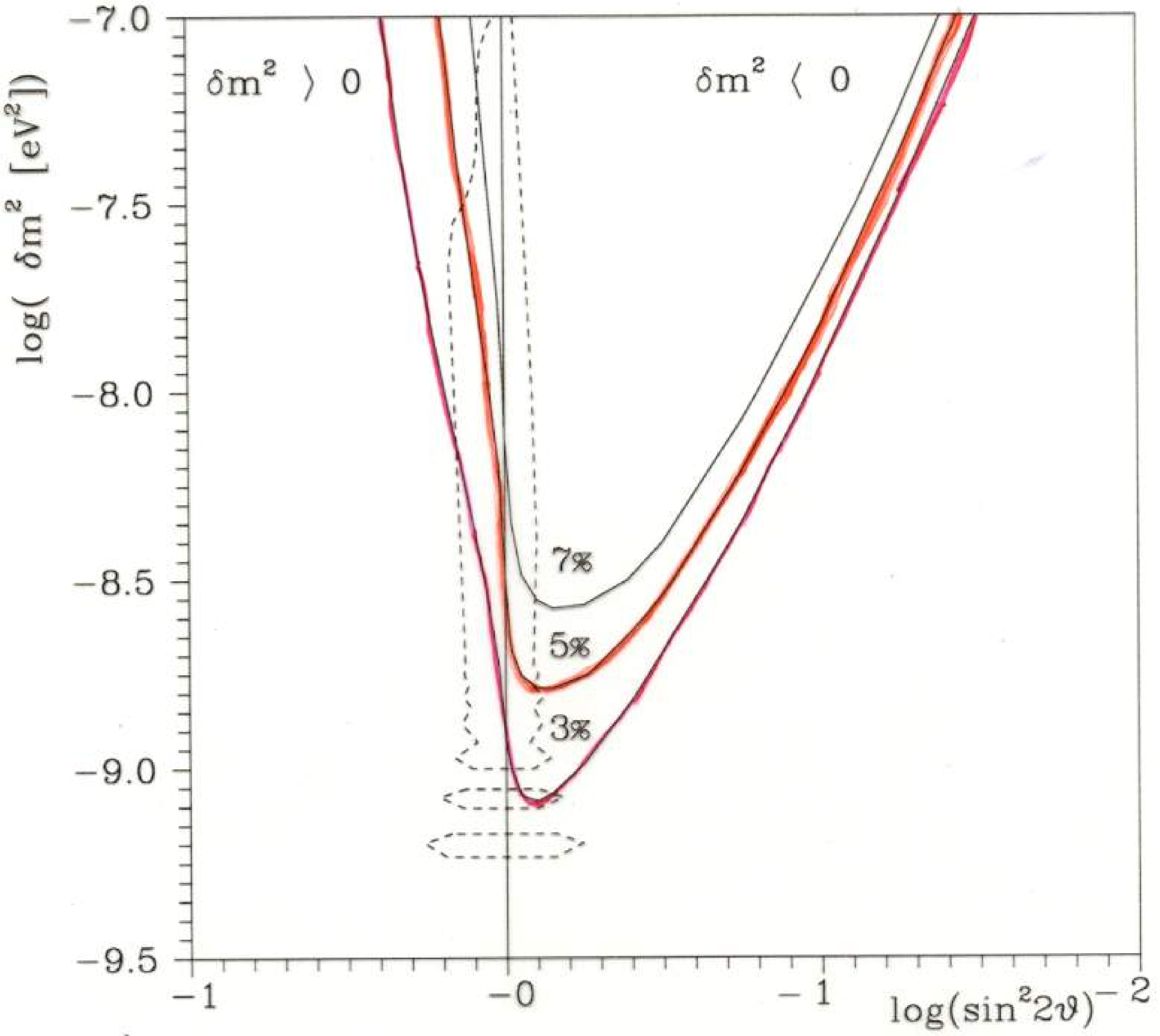

The combined iso-helium contours for the nonresonant and the resonant case of electron–sterile oscillation parameters, corresponding to different values of relative increase of helium-4, namely $\delta Y_p = (Y_{osc} - Y_p)/Y_p = 3\%, 5\%, 7\%$.

$\frac{\delta Y_p}{Y_p} \leq 3\%$

$\delta m^2 (\sin^2 2\theta)^4 \leq 1.5 \times 10^{-9}\ eV^2$ $\quad \delta m^2 > 0$

$|\delta m^2| < 8.2 \times 10^{-10}\ eV^2$ at large θ, $\delta m^2 < 0$

Updated constraints on nonresonant and resonant $\nu_e \leftrightarrow \nu_s$ assuming the conventional observational bound on $\delta Y_p/Y_p = 3\%$

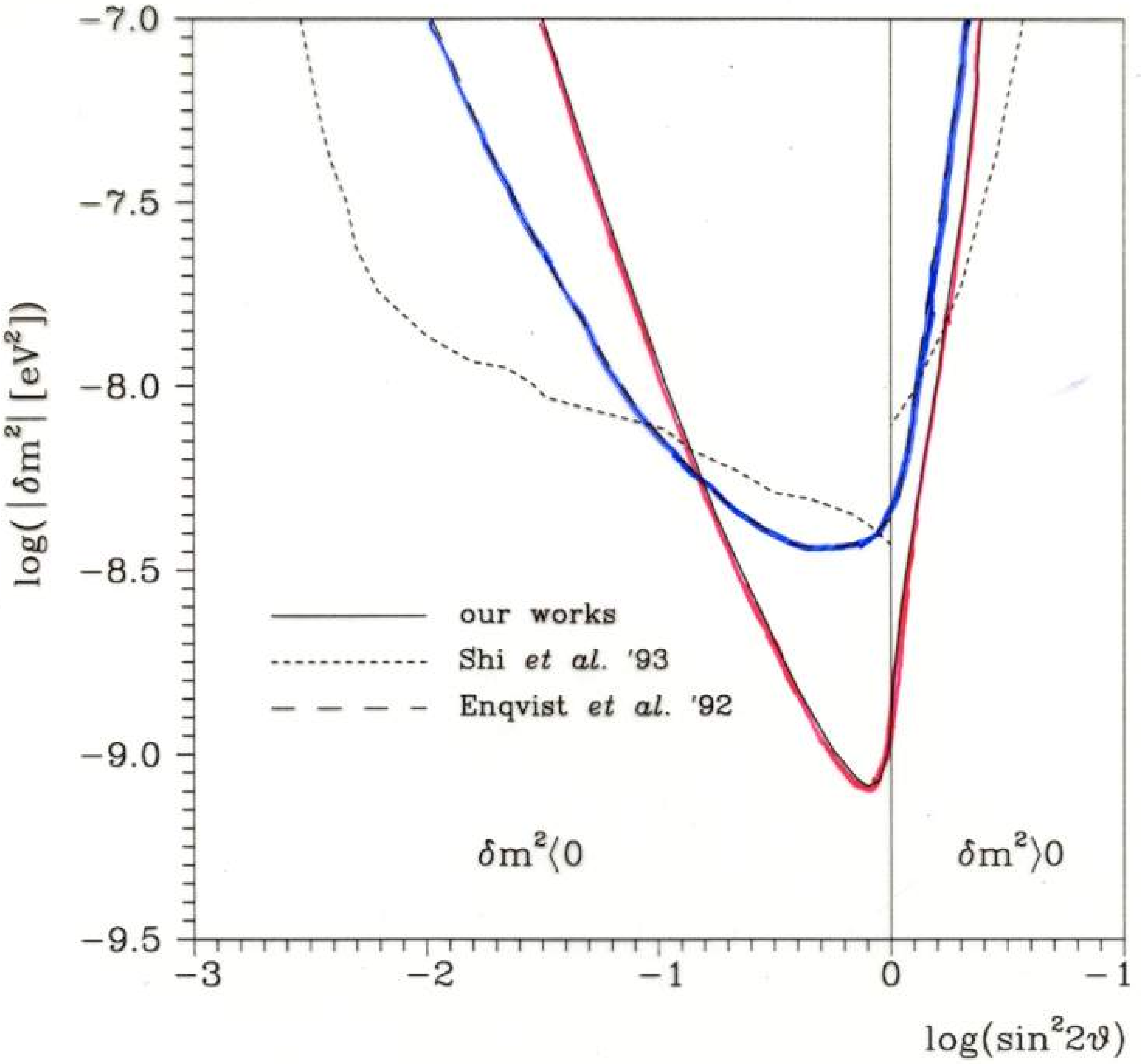

$$\delta m^2 (\sin^2 2\vartheta)^4 \leq 1.5 \times 10^{-9} \mathrm{eV}^2 \quad \delta m^2 > 0$$
$$|\delta m^2| < 8.2 \times 10^{-10} \mathrm{eV}^2 \quad \delta m^2 < 0, \quad large \;\; \vartheta,$$

The constraints are an order of magnitude stronger at large mixings than the previous due to the precise account of neutrino oscillations effects.

In the resonant case they are less restrictive at small mixings, due to the account of neutrino-antineutrino asymmetry generated in oscillations.

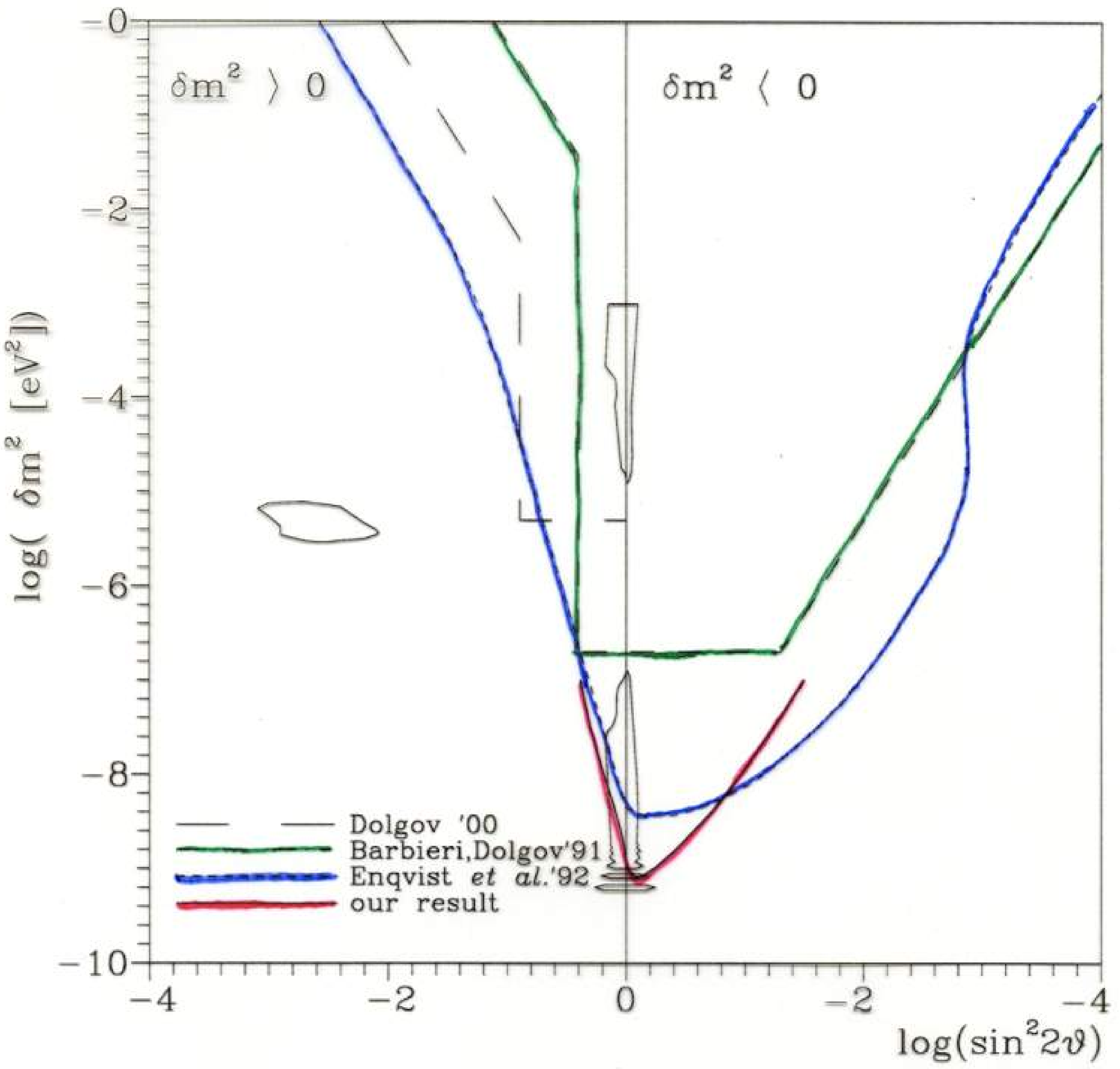

Comparison between the latest constraints and these from previous analytical and numerical analysis. LOW electron–sterile solar solution, obtained from the analysis of the 1258 days SuperKamiokande experimental data is shown in the figure by the closed dashed curves.

LMA sterile solution is excluded.

LOW sterile solution is severely constrained.
This result is consistent with the global analysis of the neutrino data from SuperKamiokande, GALLEX+GNO, SAGE and Chlorine experiments, which does not favour $\nu_e \leftrightarrow \nu_s$ LOW solution.
Bahcall J., Krastev P. and Smirnov A., hep-ph/0103179 (2001); Fukuda S.et al., hep-ex/0103033 (2001)

Hopefully new precision data on helium-4 will allow using the 1% contour and strengthen the constraints.

(a)

(b)

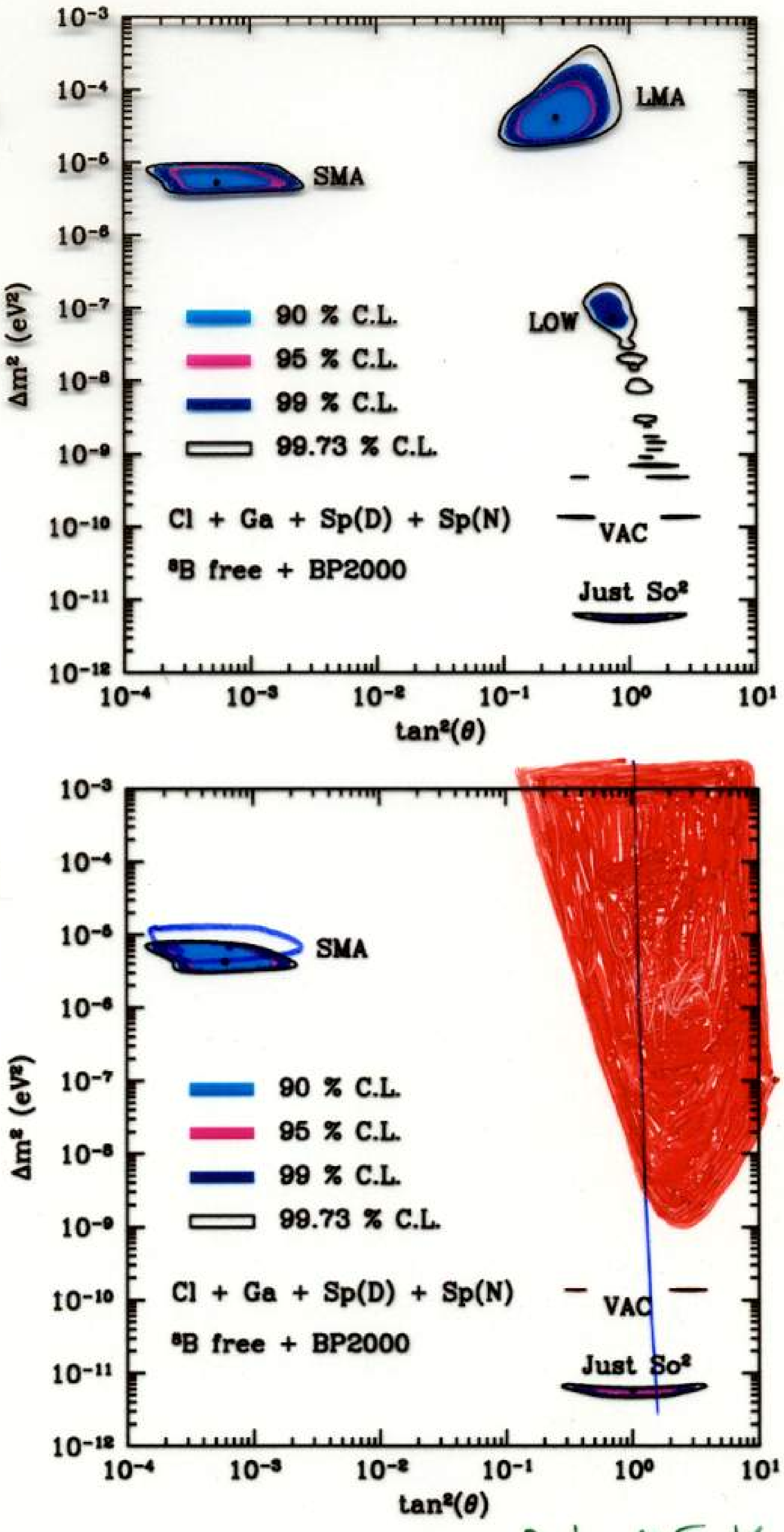

Bahcall J., Krastev P., Smirnov A.
hep-ph/0103179 , 2001

Figure 1: Global solutions, free ^{8}B and *hep* fluxes. (a) Active neutrinos. (b) Sterile neutrinos. The input data include the total rates measured in the Homestake, SAGE, and GALLEX + GNO experiments and the electron recoil energy spectrum measured by Super-Kamiokande during the day and also the spectrum measured at night. The best-fit points are marked by dark circles; the allowed regions are shown at 90%, 95%, 99%, and 99.73% C.L. .

Present and future exclusion regions

C. Albright et al., hep-ex/0008064

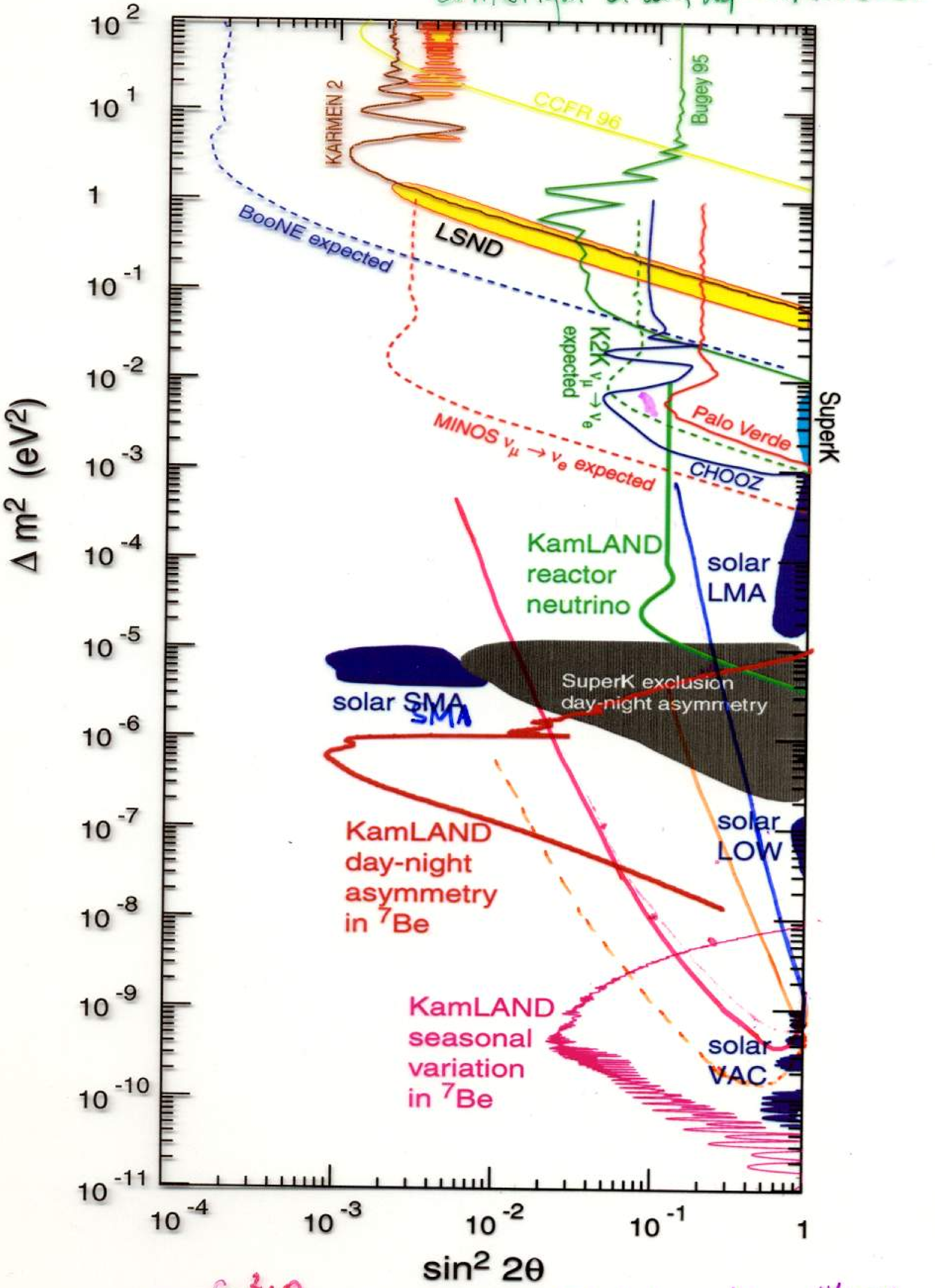

$\delta m^2 < 0$

$\delta m^2 > 0$ Present-day BBN bounds $\frac{\Delta Y}{Y} \leq 3\%$

Expected $\Delta Y/Y \leq 1\%$

Conclusions

Cosmology constrains ν oscillations strongly due to He-4 overproduction in BBN with oscillations

- flavor oscillations - not constrained ($\Delta Y_p \leq 10^{-3}$)

- active-sterille - strongly constrained

$\boxed{\nu_{\mu,\tau} \leftrightarrow \nu_s}$ - not updated for spectrum distorsion and asymmetry growth effects on He-4 $\left(\frac{\Delta Y_p^{max}}{Y_p} \leq 5\%\right)$

$|\delta m^2| (\sin^2 2\theta)^{1.8} \leq 10^{-8}\ eV^2$ $\quad \delta m^2 < 0$

$\delta m^2 \sin^4 2\theta < 3.3 . 10^{-4} \delta N_\nu^2$ $\quad \delta m^2 > 0$

$\boxed{\nu_e \leftrightarrow \nu_s}$ $\quad \left(\frac{\Delta Y_p^{max}}{Y_p} \leq 34\%, \delta m^2 < 0 ; \frac{\Delta Y_p^{max}}{Y_p} \leq 14\%, \delta m^2 > 0\right)$

$\delta m^2 \leq 8.2\ 10^{-10} eV^2$ $\quad \delta m^2 < 0$, maximal mixing

$\delta m^2 (\sin^2 2\theta)^4 \leq 1.5 . 10^{-9} eV^2$ $\quad \delta m^2 > 0$

$\frac{\Delta Y_p}{Y_p} \leq 3\%$

- The stronger $\nu_e \leftrightarrow \nu_s$ constraints are due to additional oscillation effects - ν_e depletion and spectrum distorsion.

- **LMA** and **LOW** solar oscillation $\nu_e \leftrightarrow \nu_s$ solutions and $\nu_\mu \leftrightarrow \nu_s$ atmospheric solution are excluded

- Precision determination of ^{4}He $\frac{\Delta Y_p}{Y_p} \leq 1\%$ will tighten considerably these bounds

- Relaxation of the constraints is possible $\underbrace{}_{\text{at large } \theta}$ if lepton asymmetry was present during BBN

- Cosmology gives the most stringent bound on neutrino mass differences

- Cosmological constraints on LMA (dating from 1984) and on LOW (obtained in 1999) are in remarkable agreement with the recent global analysis of experimental data

Relaxation of CN constraints

HIGHER Y_p

$\Delta Y_p \sim 0.007$

Having in mind the large systematic error of Y_p extracted from observations, $Y_p \geq 0.245$ looks possible.
We have calculated iso-helium contours $Y_p = 0.245, 0.25$ and compared them with the LOW solution.
CN constraints are relaxed, however, even $Y_p = 0.25$ cannot remove completely the constraints on LOW solution.

RELIC LEPTON ASYMMETRY L

$L \gg 10^{-10}$

Small asymmetries $L \ll 0.01$ that do not effect directly CN kinetics, influence CN *indirectly* via oscillations:
(a) effecting neutrino number densities
(b) neutrino spectrum distortion and
(c) neutrino oscillation pattern (suppressing or enhancing oscillations).

Depending on its value L reflects in suppressing or enhancing oscillations and subsequent underproduction or overproduction of ^{4}He in comparison with the case without L.

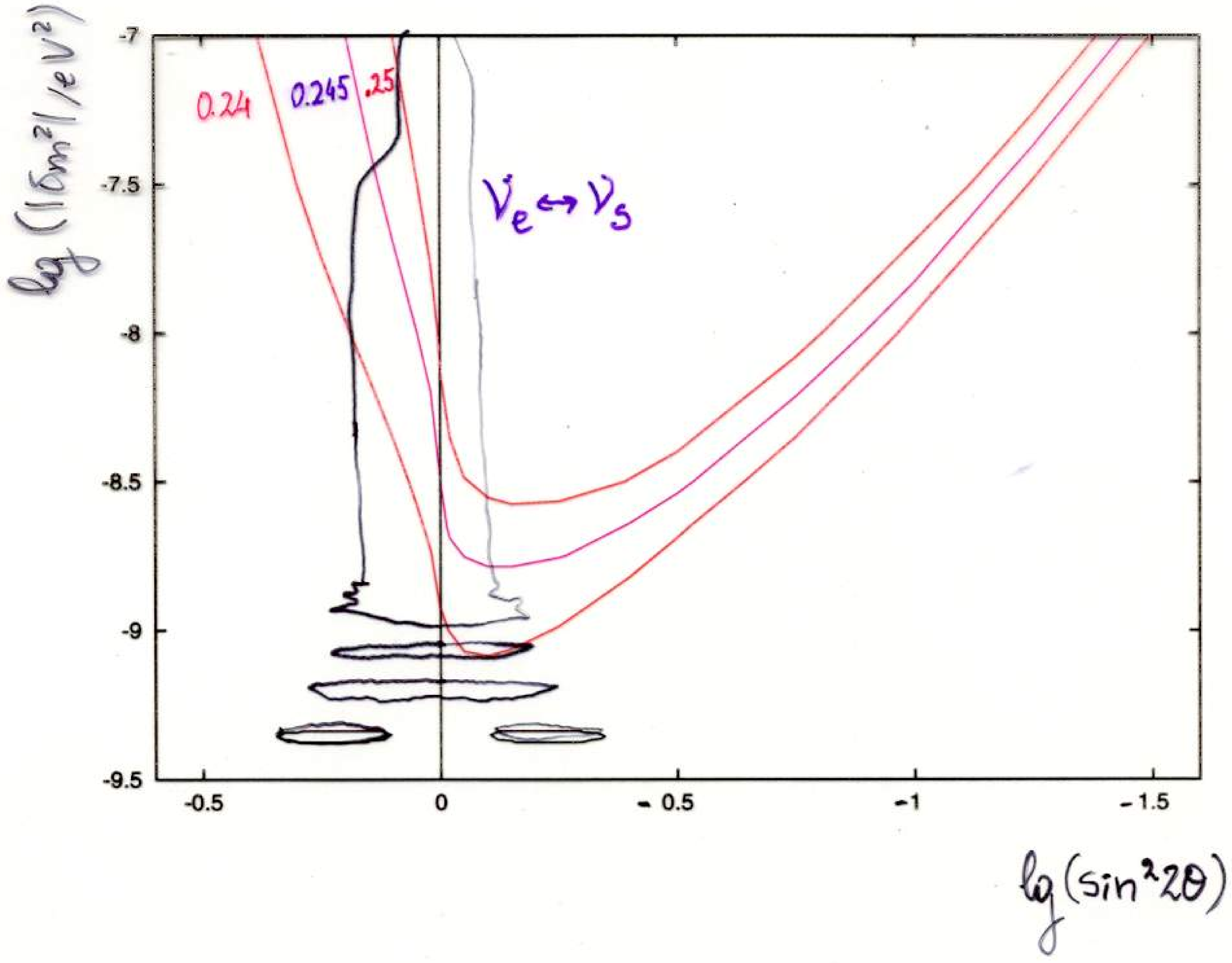

$\lg(|\delta m^2|/eV^2)$
-7
-7.5
-8
-8.5
-9
-9.5
0.24
0.245
.25
$\nu_e \leftrightarrow \nu_s$
-0.5
0
- 0.5
-1
- 1.5
$\lg(\sin^2 2\theta)$

Lepton asymmetry may both relax and tighten nucleosynthesis bounds on neutrino mixing parameters

Kirilova & Chizhov '98

Nucl. Phys. B '98

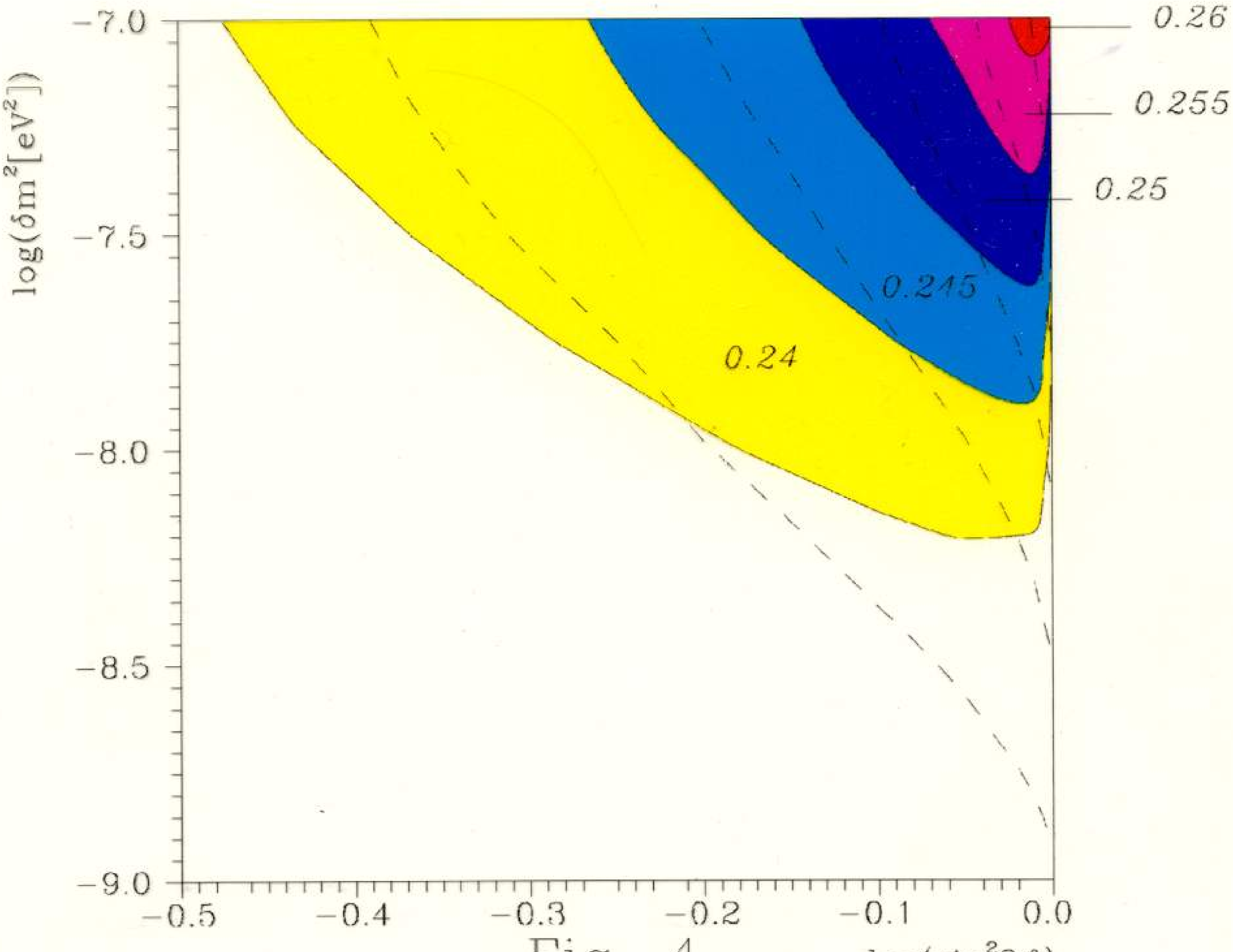

Fig. 4

Constant He-4 contours in cosmological nucleosynthesis with $\nu_e \leftrightarrow \nu_s$ for different lepton asymmetry

---- $L \simeq B$, — $L = 10^{-6}$

Dependence of $\frac{\Delta Y_p}{Y_p}$ on the initial asymmetry

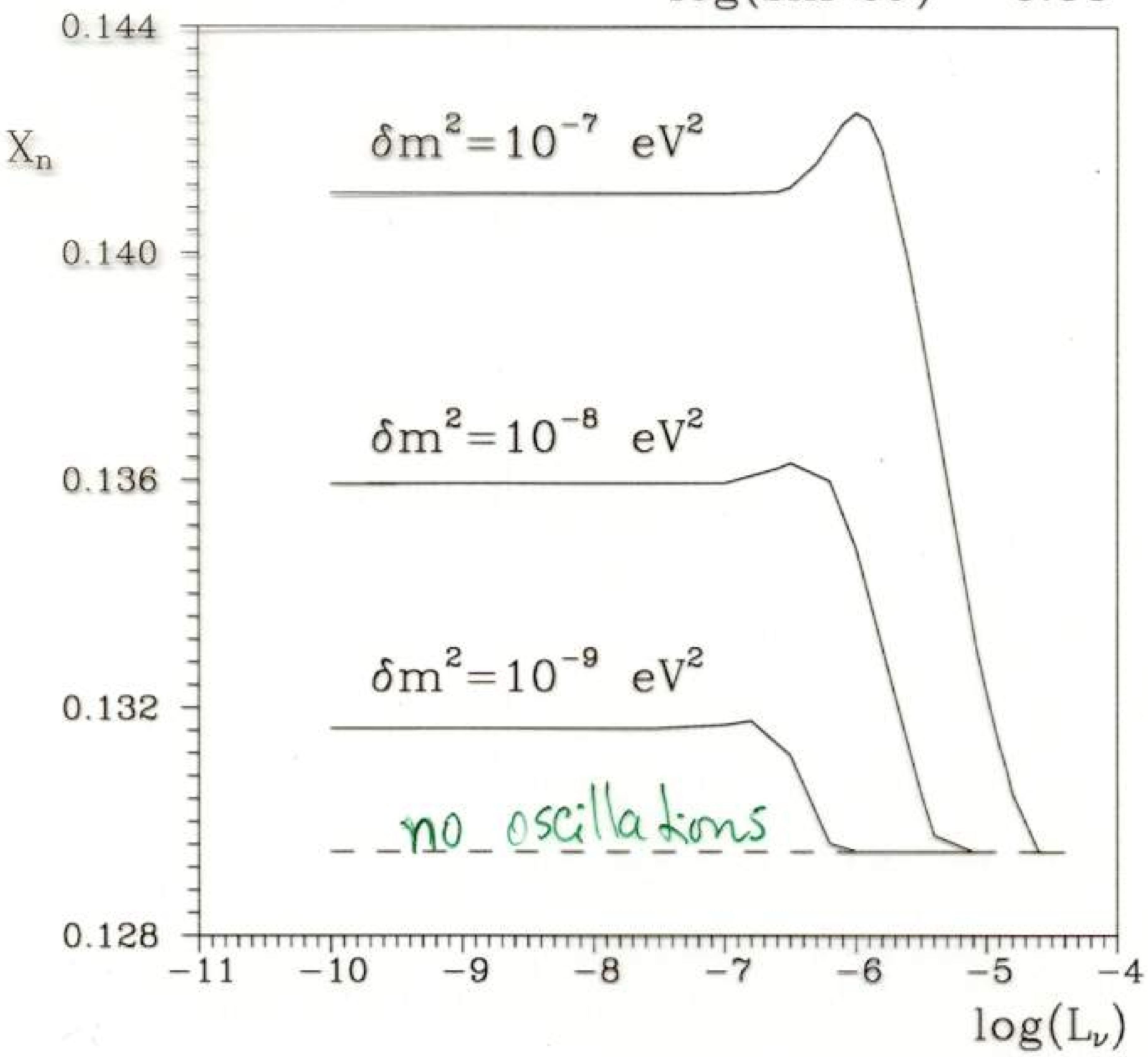

D.P.K, M.Chizhov, Nucl.Phys.B '98

Isohelium contours for different L: $L = 10^{-6}$ and $L = 10^{-10}$:

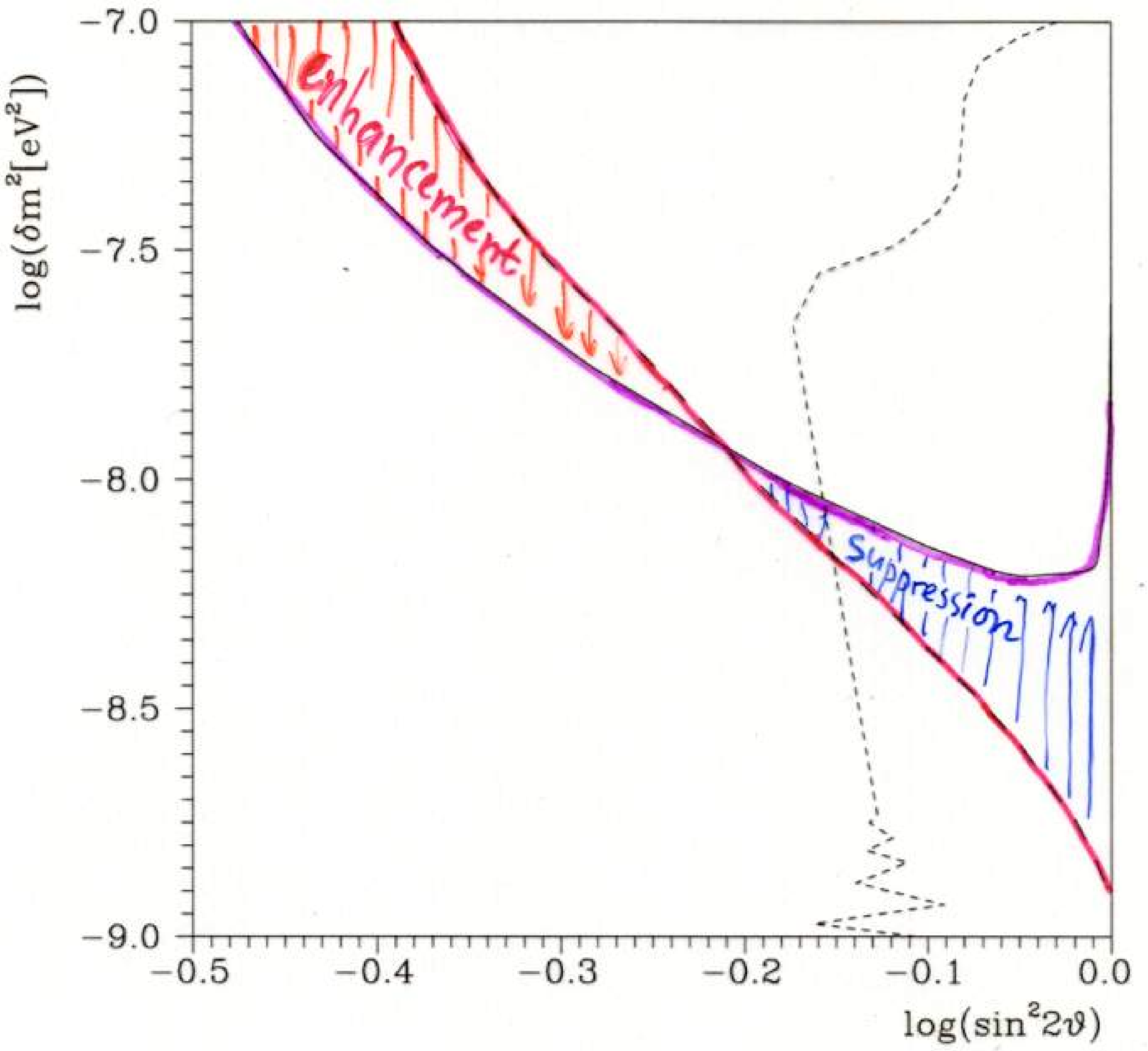

D.P.K, M.Chizhov, Nucl.Phys.B S, 2001

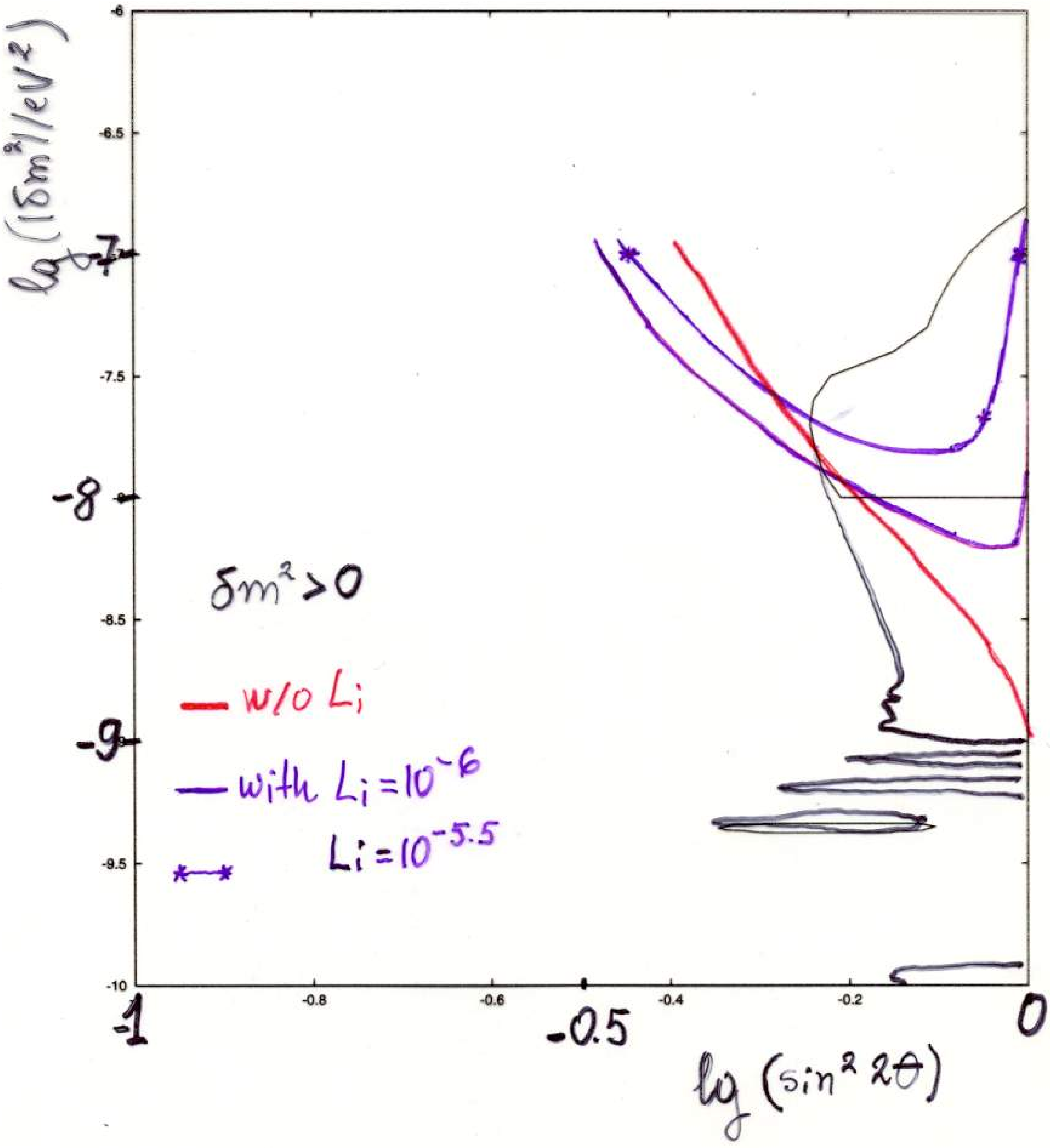

$\log(|\delta m^2|/eV^2)$
-6
-6.5
-7
-7.5
-8
-8.5
-9
-9.5
-10
$\delta m^2 > 0$
w/o L_i
with $L_i = 10^{-6}$
$L_i = 10^{-5.5}$
-1
-0.8
-0.6
-0.5
-0.4
-0.2
0
$\log(\sin^2 2\theta)$

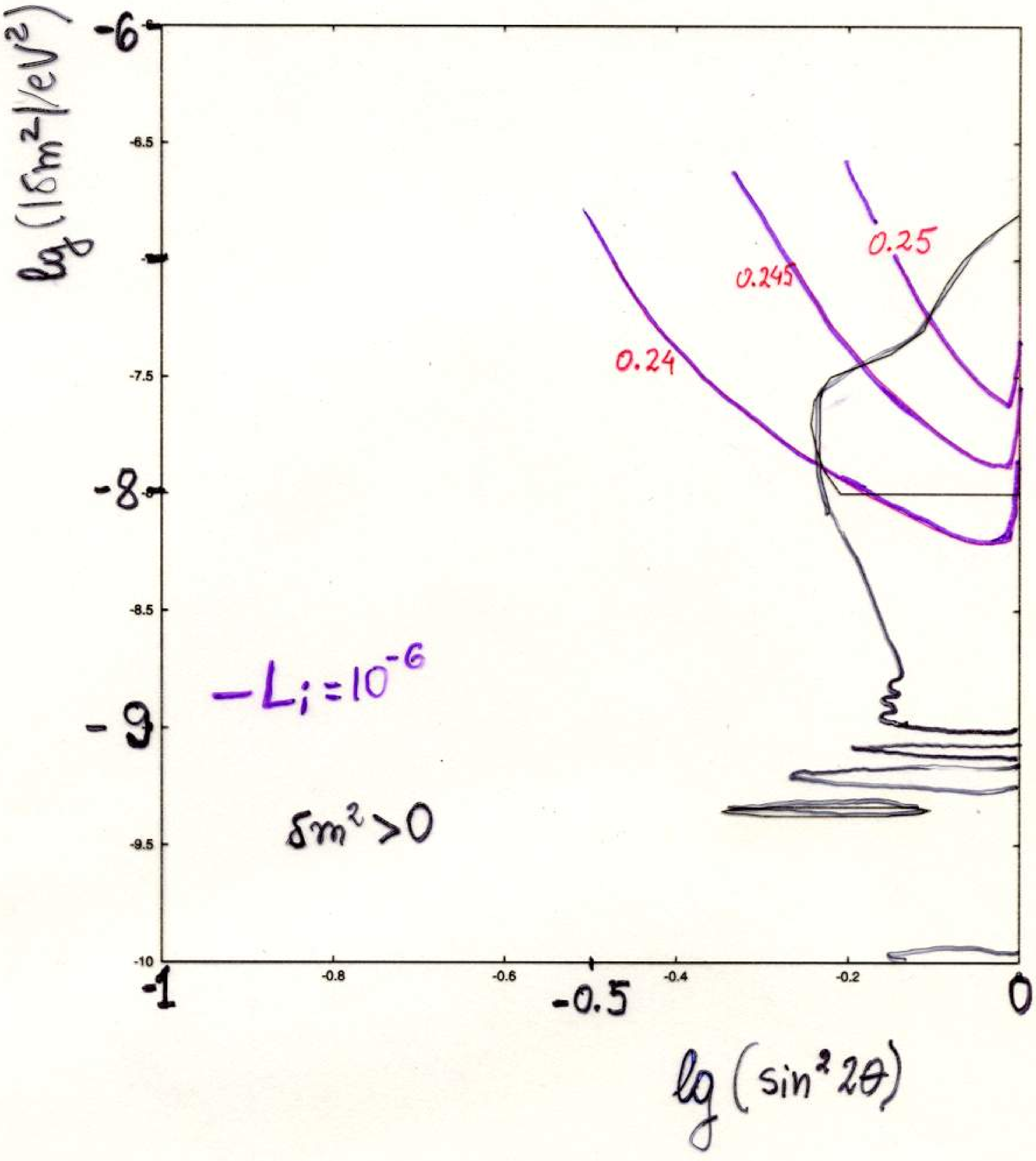

$\lg(|\delta m^2|/eV^2)$
-6
-6.5
-7.5
-8
-8.5
-9
-9.5
-10
0.25
0.245
0.24
$-L_i = 10^{-6}$
$\delta m^2 > 0$
-1
-0.8
-0.6
-0.5
-0.4
-0.2
0
$\lg(\sin^2 2\theta)$

At small mixing angles the asymmetry $L = 10^{-6}$ enhances oscillations, causing greater overproduction of He-4 and strongly constraining oscillation parameters.
At large mixings this asymmetry suppresses oscillations and leads to an underproduction of He-4 in comparisson with the case without asymmetry, thus relaxing CN bounds.

The numerical analysis showed that $L = 10^{-6}, 10^{-5.5}$ relax, while $L = 10^{-5}$ removes CN constraints on LOW solution.
D.P.K., Chizhov M.V., Nucl. Phys. B Suppl.100,360 (2001).

OSCILLATIONS GENERATED ASYMMETRY.

Lepton asymmetry can be dynamically generated due to resonant oscillations. Oscillations generated asymmetry can suppress oscillations and alleviate CN constraints.

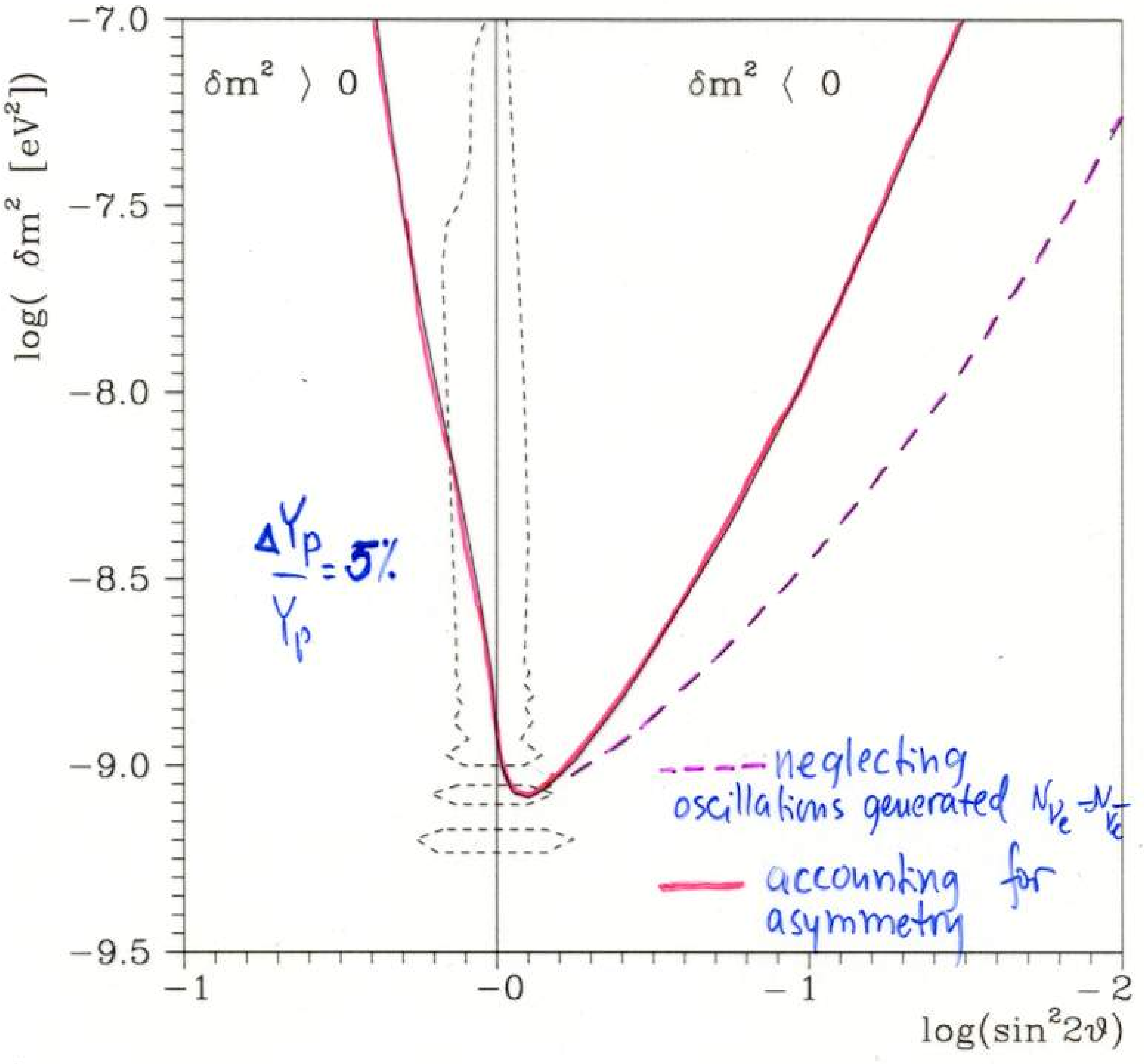

- how large asymmetry ? D.P.K, CAPP2000 proc.
- self consistent account for asymmetry and ν and nucleons evolution
- spectral distorsion is essential - a precise account needed